The University of
Nottingham

UNITED KINGDOM · CHINA · MALAYSIA

Congreve, Scott and Houston, Paul (2014) Two-grid hp-version discontinuous Galerkin finite element methods for quasi-Newtonian fluid flows. International Journal of Numerical Analysis and Modeling, 11 (3). pp. 496-524. ISSN 1705-5105

Access from the University of Nottingham repository:
http://eprints.nottingham.ac.uk/29671/1/paper_v4.pdf

TWO-GRID hp-VERSION DISCONTINUOUS GALERKIN FINITE ELEMENT METHODS FOR QUASI-NEWTONIAN FLUID FLOWS

SCOTT CONGREVE AND PAUL HOUSTON

Abstract. In this article we consider the *a priori* and *a posteriori* error analysis of two-grid hp-version discontinuous Galerkin finite element methods for the numerical solution of a strongly monotone quasi-Newtonian fluid flow problem. The basis of the two-grid method is to first solve the underlying nonlinear problem on a coarse finite element space; a fine grid solution is then computed based on undertaking a suitable linearization of the discrete problem. Here, we study two alternative linearization techniques: the first approach involves evaluating the nonlinear viscosity coefficient using the coarse grid solution, while the second method utilizes an incomplete Newton iteration technique. Energy norm error bounds are deduced for both approaches. Moreover, we design an hp-adaptive refinement strategy in order to automatically design the underlying coarse and fine finite element spaces. Numerical experiments are presented which demonstrate the practical performance of both two–grid discontinuous Galerkin methods.

Key words. hp-finite element methods; discontinuous Galerkin methods, a posteriori error estimation, adaptivity, two-grid methods, non-Newtonian fluids

1. Introduction

The purpose of this article is to develop the *a priori* and *a posteriori* error analysis of two-grid hp-version discontinuous Galerkin finite element methods (DGFEMs) for the numerical approximation of strongly monotone quasi-Newtonian fluid flow problems. The general philosophy of two-grid methods is to first approximate the underlying nonlinear problem on a coarse finite element partition of the computational domain. On the basis of this coarse grid approximation, a linearized variant of the discrete problem is then computed on a fine mesh; see, for example, [4, 8, 9, 16, 23, 27, 30, 31, 32, 33], and the references cited therein. The linearization required for the construction of the linear problem to be solved on the fine mesh may be undertaken in a number of different ways. Indeed, a simple approach is to evaluate the nonlinear coefficients arising in the underlying partial differential equation using the coarse grid approximation; in this way, the fine grid approximation essentially includes an underlying modelling or data approximation error stemming from *fixing* the data of the problem, cf. [9, 33], for example. On the other hand, the coarse grid solution may be used as the initial guess for a Newton solver on the fine mesh; in this setting, one step of the Newton iteration technique is typically undertaken, cf. [4, 33]. In the context of DGFEMs, Bi & Ginting [9] studied the first approach for a class of quasilinear elliptic PDEs, where the nonlinear diffusion coefficient μ depends on the analytical solution u; this analysis was then extended to consider the case when $\mu = \mu(|\nabla u|)$ in [15]. The analysis of DGFEMs using the two-grid technique based on employing a single step of a Newton solver for this latter class of scalar PDEs has been studied in [12].

In this article we generalize the analysis presented in [12, 14, 15] for two-grid hp-version interior penalty (IP) DGFEM approximations of scalar quasilinear elliptic

PDEs to the following non-Newtonian fluid flow problem:

$$(1) \qquad -\nabla \cdot \{\mu\left(\boldsymbol{x}, |\underline{e}\left(\boldsymbol{u}\right)|\right)\underline{e}\left(\boldsymbol{u}\right)\} + \nabla p = \boldsymbol{f} \qquad \text{in } \Omega,$$

$$(2) \qquad \nabla \cdot \boldsymbol{u} = 0 \qquad \text{in } \Omega,$$

$$(3) \qquad \boldsymbol{u} = \boldsymbol{0} \qquad \text{on } \Gamma.$$

Here, $\Omega \subset \mathbb{R}^d$, $d = 2, 3$, is a bounded polygonal, or polyhedral, Lipschitz domain with boundary $\Gamma = \partial\Omega$, $\boldsymbol{f} \in L^2(\Omega)^d$ is a given source term, $\boldsymbol{u} = (u_1, \ldots, u_d)^\top$ is the velocity vector, p is the pressure, and $\underline{e}(\boldsymbol{u})$ is the symmetric $d \times d$ strain tensor defined by

$$e_{ij}(\boldsymbol{u}) = \frac{1}{2}\left(\frac{\partial u_i}{\partial x_j} + \frac{\partial u_j}{\partial x_i}\right), \qquad i, j = 1 \ldots d.$$

Furthermore, $|\underline{e}(\boldsymbol{u})|$ is the Frobenius norm of $\underline{e}(\boldsymbol{u})$. For the purposes of this article we assume that the function μ satisfies the following structural hypothesis.

Assumption 1. We assume that the nonlinearity $\mu \in \mathrm{C}(\bar{\Omega} \times [0, \infty))$ and there exists positive constants m_μ and M_μ such that

$$(4) \qquad m_\mu(t - s) \leq \mu(\boldsymbol{x}, t)t - \mu(\boldsymbol{x}, s)s \leq M_\mu(t - s), \qquad t \geq s \geq 0, \quad \boldsymbol{x} \in \bar{\Omega}.$$

As a direct consequence of (4), we note that μ satisfies the following inequalities: there exists positive constants C_1 and C_2, such that for all $\underline{\tau}, \underline{\omega} \in \mathbb{R}^{d \times d}$ and all $\boldsymbol{x} \in \bar{\Omega}$,

$$(5) \qquad |\mu(\boldsymbol{x}, |\underline{\tau}|)\underline{\tau} - \mu(\boldsymbol{x}, |\underline{\omega}|)\underline{\omega}| \leq C_1|\underline{\tau} - \underline{\omega}|,$$

$$(6) \qquad C_2|\underline{\tau} - \underline{\omega}|^2 \leq (\mu(\boldsymbol{x}, |\underline{\tau}|)\underline{\tau} - \mu(\boldsymbol{x}, |\underline{\omega}|)\underline{\omega}) : (\underline{\tau} - \underline{\omega}).$$

For ease of notation we suppress the dependence of μ on $\boldsymbol{x}$ and write $\mu(t)$ instead of $\mu(\boldsymbol{x}, t)$. Throughout this paper, we use the following standard notation. Given $D \subset \mathbb{R}^d, d \geq 1$, a bounded Lipschitz domain, we write $H^t(D)$ to denote the usual Sobolev space of real-valued functions of order $t \geq 0$ with norm $\|\cdot\|_{H^t(D)}$; for $t = 0$, we set $L^2(D) = H^0(D)$. We write $H^1_0(D)$ to denote the subspace of functions in $H^1(D)$ with zero trace on ∂D, and set $L^2_0(D) = \{q \in L^2(D) : \int_D q \, d\boldsymbol{x} = 0\}$.

This article is organized as follows. In Section 2 we formulate the standard (single grid) IP DGFEM for the numerical approximation of the boundary-value problem (1)–(3). Sections 3 and 4 develop the *a priori* and *a posteriori* error analysis of the above mentioned variants of the two–grid hp-version IP DGFEM. On the basis of the *a posteriori* error bounds established in this article, in Section 5 we consider the design of an hp-adaptive finite element algorithm capable of automatically enriching the underlying coarse and fine finite element spaces; the performance of this adaptive strategy is studied in Section 6. Finally, in Section 7 we summarise the main results of this article and draw some conclusions.

2. hp-Version IP DGFEM approximation

In order to construct the two-grid IP DGFEMs considered in this article, we first recall the family of IP DGFEMs introduced and analysed in [13]. To this end, we introduce the following notation. Let $\mathcal{T}_h$ denote a shape-regular quadrilateral/hexahedral partition of the computational domain Ω into disjoint open-element domains κ such that $\overline{\Omega} = \bigcup_{\kappa \in \mathcal{T}_h} \overline{\kappa}$. We assume that each $\kappa \in \mathcal{T}_h$ is an affine image of a fixed master element $\widehat{\kappa}$; i.e., for each $\kappa \in \mathcal{T}_h$, there exists an affine mapping $T_\kappa : \widehat{\kappa} \to \kappa$ such that $\kappa = T_\kappa(\widehat{\kappa})$, where $\widehat{\kappa} = (-1, 1)^d$ is the reference element.

We write h_κ to denote the element diameter of $\kappa \in \mathcal{T}_h$, and set $h = \max_{\kappa \in \mathcal{T}_h} h_\kappa$; furthermore, $\boldsymbol{n}_\kappa$ signifies the unit outward normal vector to κ. We allow the meshes $\mathcal{T}_h$ to be one-irregular and assume that the family of meshes $\{\mathcal{T}_h\}_{h>0}$ is of 'bounded local variation', i.e., there exists a constant $\rho_1 \geq 1$, independent of element sizes, such that

$$(7) \qquad\qquad \rho_1^{-1} \leq h_\kappa / h_{\kappa'} \leq \rho_1$$

for any pair of elements $\kappa, \kappa' \in \mathcal{T}_h$ which share a common face $F = \partial\kappa \cap \partial\kappa'$.

Given $\kappa \in \mathcal{T}_h$, we write $k_\kappa \geq 1$ to denote the local polynomial degree; we set $\boldsymbol{k} = \{k_\kappa : \kappa \in \mathcal{T}_h\}$ and $k_{\max} = \max_{\kappa \in \mathcal{T}_h} k_\kappa$. By construction, we assume that $\boldsymbol{k}$ is also of bounded local variation, i.e., there exists a constant $\rho_2 \geq 1$, independent of the element sizes and $\boldsymbol{k}$, such that, for any pair of neighbouring elements $\kappa, \kappa' \in \mathcal{T}_h$,

$$(8) \qquad\qquad \rho_2^{-1} \leq k_\kappa / k_{\kappa'} \leq \rho_2.$$

We define the finite element spaces

$$\boldsymbol{V}(\mathcal{T}_h, \boldsymbol{k}) = \left\{ \boldsymbol{v} \in L^2(\Omega)^d : \boldsymbol{v}|_\kappa \circ T_\kappa \in \mathcal{Q}_{k_\kappa}(\widehat{\kappa})^d, \kappa \in \mathcal{T}_h \right\},$$
$$Q(\mathcal{T}_h, \boldsymbol{k}) = \left\{ q \in L_0^2(\Omega) : q|_\kappa \circ T_\kappa \in \mathcal{Q}_{k_\kappa - 1}(\widehat{\kappa}), \kappa \in \mathcal{T}_h \right\},$$

where $\mathcal{Q}_k(\widehat{\kappa})$ denotes the set of all tensor-product polynomials on $\widehat{\kappa}$ of degree k in each coordinate direction.

We write $\mathcal{F}_h^{\mathcal{I}}$ to denote the set of all interior faces, $\mathcal{F}_h^{\mathcal{B}}$ the set of all boundary faces and $\mathcal{F}_h = \mathcal{F}_h^{\mathcal{I}} \cup \mathcal{F}_h^{\mathcal{B}}$ the set of all faces associated with the mesh $\mathcal{T}_h$. Given two adjacent elements, $\kappa^+, \kappa^- \in \mathcal{T}_h$, which share a common face $F \in \mathcal{F}_h^{\mathcal{I}}$, i.e., $F = \partial\kappa^+ \cap \partial\kappa^-$, for scalar-, vector- and matrix-valued functions, q, $\boldsymbol{v}$, and $\underline{\tau}$, respectively, which are smooth inside each element $\kappa \in \mathcal{T}_h$, we write $q^\pm$, $\boldsymbol{v}^\pm$, and $\underline{\tau}^\pm$ to denote the traces of the functions q, $\boldsymbol{v}$, and $\underline{\tau}$, respectively, on the face F, taken from the interior of $\kappa^\pm$, respectively. The averages of q, $\boldsymbol{v}$, and $\underline{\tau}$ at $\boldsymbol{x} \in F$ are given by

$$\{\!\{q\}\!\} = \frac{1}{2}(q^+ + q^-), \qquad \{\!\{\boldsymbol{v}\}\!\} = \frac{1}{2}(\boldsymbol{v}^+ + \boldsymbol{v}^-), \qquad \{\!\{\underline{\tau}\}\!\} = \frac{1}{2}(\underline{\tau}^+ + \underline{\tau}^-),$$

respectively. Similarly, the jumps of q, $\boldsymbol{v}$, and $\underline{\tau}$ at $\boldsymbol{x} \in F$ are given by

$$[\![q]\!] = q^+ \boldsymbol{n}_{\kappa^+} + q^- \boldsymbol{n}_{\kappa^-}, \qquad\qquad [\![\boldsymbol{v}]\!] = \boldsymbol{v}^+ \cdot \boldsymbol{n}_{\kappa^+} + \boldsymbol{v}^- \cdot \boldsymbol{n}_{\kappa^-},$$
$$\underline{[\![\boldsymbol{v}]\!]} = \boldsymbol{v}^+ \otimes \boldsymbol{n}_{\kappa^+} + \boldsymbol{v}^- \otimes \boldsymbol{n}_{\kappa^-}, \qquad [\![\underline{\tau}]\!] = \underline{\tau}^+ \boldsymbol{n}_{\kappa^+} + \underline{\tau}^- \boldsymbol{n}_{\kappa^-}.$$

On a boundary face $F \in \mathcal{F}_h^{\mathcal{B}}$, we set $\{\!\{q\}\!\} = q$, $\{\!\{\boldsymbol{v}\}\!\} = \boldsymbol{v}$, $\{\!\{\underline{\tau}\}\!\} = \underline{\tau}$, $[\![q]\!] = q\boldsymbol{n}$, $[\![\boldsymbol{v}]\!] = \boldsymbol{v} \cdot \boldsymbol{n}$, $\underline{[\![\boldsymbol{v}]\!]} = \boldsymbol{v} \otimes \boldsymbol{n}$ and $[\![\underline{\tau}]\!] = \underline{\tau}\boldsymbol{n}$, with $\boldsymbol{n}$ denoting the unit outward normal vector on the boundary Γ.

Given a (fine) mesh $\mathcal{T}_h$, together with a corresponding polynomial degree vector $\boldsymbol{k}$, the standard IP DGFEM is defined as follows: find $(\boldsymbol{u}_{h,k}, p_{h,k}) \in \boldsymbol{V}(\mathcal{T}_h, \boldsymbol{k}) \times Q(\mathcal{T}_h, \boldsymbol{k})$ such that

$$(9) \qquad A_{h,k}(\boldsymbol{u}_{h,k}; \boldsymbol{u}_{h,k}, \boldsymbol{v}_{h,k}) + B_{h,k}(\boldsymbol{v}_{h,k}, p_{h,k}) = F_{h,k}(\boldsymbol{v}_{h,k}),$$
$$(10) \qquad\qquad\qquad\qquad -B_{h,k}(\boldsymbol{u}_{h,k}, q_{h,k}) = 0$$

for all $(\boldsymbol{v}_{h,k}, q_{h,k}) \in \boldsymbol{V}(\mathcal{T}_h, \boldsymbol{k}) \times Q(\mathcal{T}_h, \boldsymbol{k})$, where

$$A_{h,k}(\boldsymbol{\psi}; \boldsymbol{u}, \boldsymbol{v}) = \int_\Omega \mu(|\underline{e}_h(\boldsymbol{\psi})|)\underline{e}_h(\boldsymbol{u}) : \underline{e}_h(\boldsymbol{v}) \, d\boldsymbol{x} + \sum_{F \in \mathcal{F}_h} \int_F \sigma_{h,k} [\![\boldsymbol{u}]\!] : [\![\boldsymbol{v}]\!] \, ds$$

$$- \sum_{F \in \mathcal{F}_h} \int_F \{\!\{\mu(|\underline{e}_h(\boldsymbol{\psi})|)\underline{e}_h(\boldsymbol{u})\}\!\} : [\![\boldsymbol{v}]\!] \, ds$$

$$+ \theta \sum_{F \in \mathcal{F}_h} \int_F \{\!\{\mu(h_F^{-1}|[\![\boldsymbol{\psi}]\!]|)\underline{e}_h(\boldsymbol{v})\}\!\} : [\![\boldsymbol{u}]\!] \, ds,$$

$$B_{h,k}(\boldsymbol{v}, q) = \int_\Omega q \nabla_h \cdot \boldsymbol{v} \, ds + \sum_{F \in \mathcal{F}_h} \int_F \{\!\{q\}\!\} [\![\boldsymbol{v}]\!] \, ds,$$

$$F_{h,k}(\boldsymbol{v}) = \int_\Omega \boldsymbol{f} \cdot \boldsymbol{v} \, d\boldsymbol{x},$$

cf. [13]. Here, $\underline{e}_h(\cdot)$ and ∇_h denote the element-wise strain tensor and gradient operator, respectively, and $\theta \in [-1, 1]$. The *interior penalty parameter* $\sigma_{h,k}$ is defined as follows:

$$(11) \qquad\qquad \sigma_{h,k} = \gamma \frac{k_F^2}{h_F},$$

where $\gamma \geq 1$ is a constant, which must be chosen sufficiently large (independent of the local element sizes and the polynomial degree); see Lemma 2 below. Moreover, for a face $F \in \mathcal{F}_h$, $h_F = \operatorname{diam}(F)$ and the face polynomial degree k_F is defined by

$$k_F = \begin{cases} \max(k_\kappa, k_{\kappa'}), & \text{if } F = \partial\kappa \cap \partial\kappa' \in \mathcal{F}_h^\mathcal{I}, \\ k_\kappa, & \text{if } F = \partial\kappa \cap \Gamma \in \mathcal{F}_h^\mathcal{B}. \end{cases}$$

Employing (7) and (8), together with the inverse inequality derived in [25, Theorem 4.76], we deduce the following result.

Lemma 1. *There exists a positive constant* $C_T = C_T(\rho_1, \rho_2)$, *independent of the discretization parameters* h *and* $\boldsymbol{k}$, *such that*

$$\sum_{F \in \mathcal{F}_h} \int_F h_F k_F^{-2} |\{\!\{\underline{e}_h(\boldsymbol{w})\}\!\}|^2 \, ds \leq C_T \, \|\underline{e}_h(\boldsymbol{w})\|_{L^2(\Omega)}^2 \quad \text{for all} \ \ \boldsymbol{w} \in \boldsymbol{V}(\mathcal{T}_h, \boldsymbol{k}).$$

Introducing the energy norms

$$\|\boldsymbol{v}\|_{h,k}^2 = \|\underline{e}_h(\boldsymbol{v})\|_{L^2(\Omega)}^2 + \sum_{F \in \mathcal{F}_h} \int_F \sigma_{h,k} |[\![\boldsymbol{v}]\!]|^2 \, ds,$$

$$\|(\boldsymbol{v}, q)\|_{\mathrm{DG}(h,k)}^2 = \|\boldsymbol{v}\|_{h,k}^2 + \|q\|_{L^2(\Omega)}^2,$$

we note that $A_{h,k}$ is coercive in the following sense.

Lemma 2. *There exists a constant* $\gamma_{\min}$ *such that the semilinear form* $A_{h,k}(\cdot; \cdot, \cdot)$ *is coercive in the sense that there exists a positive constant* C, *independent of* h *and* $\boldsymbol{k}$, *such that*

$$A_{h,k}(\boldsymbol{\phi}; \boldsymbol{v}, \boldsymbol{v}) \geq C \, \|\boldsymbol{v}\|_{h,k}^2$$

for all $\boldsymbol{v}, \boldsymbol{\phi} \in \boldsymbol{V}(\mathcal{T}_h, \boldsymbol{k})$, *providing that the interior penalty parameter* $\gamma \geq \gamma_{\min}$.

Proof. The proof follows in an analogous fashion to the case of the scalar PDE considered in [15], albeit, based on employing the inverse inequality stated in Lemma 1; for details, see [11]. □

We assume that the bilinear form $B_{h,k}$ satisfies the following discrete inf-sup condition: there exists a positive constant ν, independent of the discretization parameters h and $\boldsymbol{k}$, such that

$$(12) \qquad \inf_{0 \neq q \in Q(\mathcal{T}_h, \boldsymbol{k})} \sup_{\boldsymbol{0} \neq \boldsymbol{v} \in \boldsymbol{V}(\mathcal{T}_h, \boldsymbol{k})} \frac{B_{h,k}(\boldsymbol{v}, q)}{\|\boldsymbol{v}\|_{h,k} \|q\|_{L^2(\Omega)}} \geq \nu k_{\max}^{-1}.$$

We note that this inf-sup condition holds

- for $k_\kappa \geq 2$, $\kappa \in \mathcal{T}_h$, or
- for $k \geq 1$ if $\mathcal{T}_h$ is conforming and $k_\kappa = k$ for all $\kappa \in \mathcal{T}_h$;

see Theorem 6.2 and Theorem 6.12, respectively, in [24]. Exploiting this condition it can be shown that the formulation (9)–(10) is well-posed, see [13]. Furthermore, the following *a priori* error bound holds (see [13, Theorem 4.1]).

Theorem 3. *Let the penalty parameter γ be sufficiently large, and assume that the solution $(\boldsymbol{u}, p)$ of (1)–(3) belong to $(C^1(\Omega) \cap H^2(\Omega))^d \times (C^0(\Omega) \cap H^1(\Omega))$, and $\boldsymbol{u}|_\kappa \in H^{s_\kappa}(\kappa)^d$, $p|_\kappa \in H^{s_\kappa - 1}(\kappa)$, $s_\kappa \geq 2$, $\kappa \in \mathcal{T}_h$. Then, provided that the discrete inf-sup condition (12) is valid, the following estimate holds*

$$\|(\boldsymbol{u} - \boldsymbol{u}_h, p - p_h)\|_{\mathrm{DG}(h,k)}^2$$
$$\leq C k_{\max}^4 \sum_{\kappa \in \mathcal{T}_h} \left(\frac{h_\kappa^{2\min\{s_\kappa, k_\kappa+1\}-2}}{k_\kappa^{2s_\kappa - 3}} \|\boldsymbol{u}\|_{H^{s_\kappa}(\kappa)}^2 + \frac{h_\kappa^{2\min\{s_\kappa, k_\kappa+1\}-2}}{k_\kappa^{2s_\kappa - 2}} \|p\|_{H^{s_\kappa - 1}(\kappa)}^2 \right),$$

where $(\boldsymbol{u}_h, p_h)$ is the IP DGFEM solution defined in (9)–(10), and the constant $C > 0$ is independent of the mesh size and the polynomial degrees.

3. Two-grid hp-Version IP DGFEM

In this section we develop a two-grid version of the IP DGFEM for the numerical approximation of (1)–(3) based on the formulation proposed in [9, 14, 15]. To this end, we consider a fine and coarse partition of the computational domain Ω, denoted by $\mathcal{T}_h$ and $\mathcal{T}_H$, respectively, which we assume are nested in the sense that, for any $\kappa_h \in \mathcal{T}_h$ there exists a $\kappa_H \in \mathcal{T}_H$ such that $\bar{\kappa}_h \subseteq \bar{\kappa}_H$. Moreover we define the polynomial degree vectors $\boldsymbol{k} = \{k_\kappa : \kappa \in \mathcal{T}_h\}$ and $\boldsymbol{K} = \{K_\kappa : \kappa \in \mathcal{T}_H\}$, associated with the meshes $\mathcal{T}_h$ and $\mathcal{T}_H$, respectively, with the property that, given $\kappa_h \in \mathcal{T}_h$ and the associated $\kappa_H \in \mathcal{T}_H$, such that $\bar{\kappa}_h \subseteq \bar{\kappa}_H$, the corresponding elemental polynomial degrees satisfy the condition that $k_{\kappa_h} \geq K_{\kappa_H}$. Equipped with $\mathcal{T}_h$, $\boldsymbol{k}$ and $\mathcal{T}_H$, $\boldsymbol{K}$, we define the corresponding fine and coarse hp-finite element spaces $\boldsymbol{V}(\mathcal{T}_h, \boldsymbol{k})$, $Q(\mathcal{T}_h, \boldsymbol{k})$ and $\boldsymbol{V}(\mathcal{T}_H, \boldsymbol{K})$, $Q(\mathcal{T}_H, \boldsymbol{K})$, respectively, which satisfy the inclusions: $\boldsymbol{V}(\mathcal{T}_H, \boldsymbol{K}) \subseteq \boldsymbol{V}(\mathcal{T}_h, \boldsymbol{k})$ and $Q(\mathcal{T}_H, \boldsymbol{K}) \subseteq Q(\mathcal{T}_h, \boldsymbol{k})$.

The two–grid IP DGFEM discretization of (1)–(3) is given by:

(1) (Nonlinear solve) Compute $(\boldsymbol{u}_{H,K}, p_{H,K}) \in \boldsymbol{V}(\mathcal{T}_H, \boldsymbol{K}) \times Q(\mathcal{T}_H, \boldsymbol{K})$ such that

$$(13) \qquad A_{H,K}(\boldsymbol{u}_{H,K}; \boldsymbol{u}_{H,K}, \boldsymbol{v}_{H,K}) + B_{H,K}(\boldsymbol{v}_{H,K}, p_{H,K}) = F_{H,K}(\boldsymbol{v}_{H,K}),$$

$$(14) \qquad -B_{H,K}(\boldsymbol{u}_{H,K}, q_{H,K}) = 0$$

for all $(\boldsymbol{v}_{H,K}, q_{H,K}) \in \boldsymbol{V}(\mathcal{T}_H, \boldsymbol{K}) \times Q(\mathcal{T}_H, \boldsymbol{K})$.

(2) (Linear solve) Determine the fine grid solution $(\boldsymbol{u}_{2G}, p_{2G}) \in \boldsymbol{V}(\mathcal{T}_h, \boldsymbol{k}) \times Q(\mathcal{T}_h, \boldsymbol{k})$ such that

$$(15) \qquad A_{h,k}(\boldsymbol{u}_{H,K}; \boldsymbol{u}_{2G}, \boldsymbol{v}_{h,k}) + B_{h,k}(\boldsymbol{v}_{h,k}, p_{2G}) = F_{h,k}(\boldsymbol{v}_{h,k}),$$

$$(16) \qquad\qquad\qquad\qquad -B_{h,k}(\boldsymbol{u}_{2G}, q_{h,k}) = 0$$

for all $(\boldsymbol{v}_{h,k}, q_{h,k}) \in \boldsymbol{V}(\mathcal{T}_h, \boldsymbol{k}) \times Q(\mathcal{T}_h, \boldsymbol{k})$.

The existence and uniqueness of the solution $(\boldsymbol{u}_{H,K}, p_{H,K})$ follows immediately from [13], cf. above. Since $A_{h,k}(\boldsymbol{u}_{H,K}; \cdot, \cdot)$ is coercive on $\boldsymbol{V}(\mathcal{T}_h, \boldsymbol{k}) \times \boldsymbol{V}(\mathcal{T}_h, \boldsymbol{k})$, cf. Lemma 2, the continuity of $A_{h,k}(\boldsymbol{u}_{H,K}; \cdot, \cdot)$ on $\boldsymbol{V}(\mathcal{T}_h, \boldsymbol{k}) \times Q(\mathcal{T}_h, \boldsymbol{k})$, $B_{h,k}(\cdot, \cdot)$ on $\boldsymbol{V}(\mathcal{T}_h, \boldsymbol{k}) \times Q(\mathcal{T}_h, \boldsymbol{k})$ and $F_{h,k}(\cdot)$ on $\boldsymbol{V}(\mathcal{T}_h, \boldsymbol{k})$, together with the discrete inf-sup condition (12) implies the existence and uniqueness of $(\boldsymbol{u}_{2G}, p_{2G})$, cf. [10, 17, 24, 26]. Hence, the formulation (13)–(16) is well-posed.

3.1. *A priori* error bound. In this section we deduce the following error bound for the two-grid approximation (13)–(16) of the non-Newtonian fluid flow problem (1)–(3).

Theorem 4. *Assuming that $(\boldsymbol{u}, p) \in (C^1(\Omega) \cap H^2(\Omega))^d \times (C^0(\Omega) \cap H^1(\Omega))$, $\boldsymbol{u}|_{\kappa_h} \in H^{s_{\kappa_h}}(\kappa_h)^d$, $p|_{\kappa_h} \in H^{s_{\kappa_h}-1}(\kappa_h), s_{\kappa_h} \geq 2$, for $\kappa_h \in \mathcal{T}_h$, and $\boldsymbol{u}|_{\kappa_H} \in H^{S_{\kappa_H}}(\kappa_H)^d$, $p|_{\kappa_H} \in H^{S_{\kappa_H}-1}(\kappa_H), S_{\kappa_H} \geq 2$, for $\kappa_H \in \mathcal{T}_H$, then the solution $(\boldsymbol{u}_{2G}, p_{2G}) \in \boldsymbol{V}(\mathcal{T}_h, \boldsymbol{k}) \times Q(\mathcal{T}_h, \boldsymbol{k})$ of (13)–(16) satisfies the bounds*

$$
\begin{aligned}
&\|\boldsymbol{u}_{h,k} - \boldsymbol{u}_{2G}\|_{h,k}^2 \\
(17) \quad &\leq C k_{\max}^4 \sum_{\kappa_H \in \mathcal{T}_H} \left\{ \frac{H_{\kappa_H}^{2R_{\kappa_H}-2}}{K_{\kappa_H}^{2S_{\kappa_H}-3}} \|\boldsymbol{u}\|_{H^{S_{\kappa_H}}(\kappa_H)}^2 + \frac{H_{\kappa_H}^{2R_{\kappa_H}-2}}{K_{\kappa_H}^{2S_{\kappa_H}-2}} \|p\|_{H^{S_{\kappa_H}-1}(\kappa_H)}^2 \right\},
\end{aligned}
$$

$$
\begin{aligned}
&\|p_{h,k} - p_{2G}\|_{h,k}^2 \\
(18) \quad &\leq C k_{\max}^6 \sum_{\kappa_H \in \mathcal{T}_H} \left\{ \frac{H_{\kappa_H}^{2R_{\kappa_H}-2}}{K_{\kappa_H}^{2S_{\kappa_H}-3}} \|\boldsymbol{u}\|_{H^{S_{\kappa_H}}(\kappa_H)}^2 + \frac{H_{\kappa_H}^{2R_{\kappa_H}-2}}{K_{\kappa_H}^{2S_{\kappa_H}-2}} \|p\|_{H^{S_{\kappa_H}-1}(\kappa_H)}^2 \right\},
\end{aligned}
$$

$$
\begin{aligned}
&\|(\boldsymbol{u} - \boldsymbol{u}_{2G}, p - p_{2G})\|_{\mathrm{DG}(h,k)}^2 \\
(19) \quad & \\
&\leq C k_{\max}^4 \sum_{\kappa_h \in \mathcal{T}_h} \left\{ \frac{h_{\kappa_h}^{2r_{\kappa_h}-2}}{k_{\kappa_h}^{2s_{\kappa_h}-3}} \|\boldsymbol{u}\|_{H^{s_{\kappa_h}}(\kappa_h)}^2 + \frac{h_{\kappa_h}^{2r_{\kappa_h}-2}}{k_{\kappa_h}^{2s_{\kappa_h}-2}} \|p\|_{H^{s_{\kappa_h}-1}(\kappa_h)}^2 \right\} \\
&\quad + C k_{\max}^6 \sum_{\kappa_H \in \mathcal{T}_H} \left\{ \frac{H_{\kappa_H}^{2R_{\kappa_H}-2}}{K_{\kappa_H}^{2S_{\kappa_H}-3}} \|\boldsymbol{u}\|_{H^{S_{\kappa_H}}(\kappa_H)}^2 + \frac{H_{\kappa_H}^{2R_{\kappa_H}-2}}{K_{\kappa_H}^{2S_{\kappa_H}-2}} \|p\|_{H^{S_{\kappa_H}-1}(\kappa_H)}^2 \right\},
\end{aligned}
$$

where C is a positive constant independent of $\boldsymbol{u}, p, \boldsymbol{h}, \boldsymbol{H}, \boldsymbol{k}$ and $\boldsymbol{K}$, with $1 \leq r_{\kappa_h} \leq \min(s_{\kappa_h}, k_{\kappa_h}+1), k_{\kappa_h} \geq 1$, for all $\kappa_h \in \mathcal{T}_h, 1 \leq R_{\kappa_H} \leq \min(S_{\kappa_H}, K_{\kappa_H}+1), K_{\kappa_H} \geq 1$, for all $\kappa_H \in \mathcal{T}_H$.

3.1.1. Proof of Theorem 4. In order to prove Theorem 4, we first state the following result.

Lemma 5. *Let $\boldsymbol{u}_{h,k} \in \boldsymbol{V}(\mathcal{T}_h, \boldsymbol{k})$ and $\boldsymbol{u}_{2G} \in \boldsymbol{V}(\mathcal{T}_h, \boldsymbol{k})$ be the velocity vector components of the solutions to (9)–(10) and (13)–(16), respectively, then assuming*

that $(\boldsymbol{u}, p) \in (C^1(\Omega) \cap H^2(\Omega))^d \times (C^0(\Omega) \cap H^1(\Omega))$, $\boldsymbol{u}|_{\kappa_H} \in H^{S_{\kappa_H}}(\kappa_H)^d$, $p|_{\kappa_H} \in H^{S_{\kappa_H}-1}(\kappa_H)$, $S_{\kappa_H} \geq 2$, for $\kappa_H \in \mathcal{T}_H$, then

$$A_{h,k}(\boldsymbol{u}_{H,K}; \boldsymbol{u}_{h,k}, \boldsymbol{\phi}) - A_{h,k}(\boldsymbol{u}_{h,k}; \boldsymbol{u}_{h,k}, \boldsymbol{\phi}) \leq C \|\boldsymbol{\phi}\|_{h,k} k_{\max}^2$$

$$\times \left(\sum_{\kappa_H \in \mathcal{T}_H} \left\{ \frac{H_{\kappa_H}^{2R_{\kappa_H}-2}}{K_{\kappa_H}^{2S_{\kappa_H}-3}} \|\boldsymbol{u}\|^2_{H^{S_{\kappa_H}}(\kappa_H)} + \frac{H_{\kappa_H}^{2R_{\kappa_H}-2}}{K_{\kappa_H}^{2S_{\kappa_H}-2}} \|p\|^2_{H^{S_{\kappa_H}-1}(\kappa_H)} \right\} \right)^{\frac{1}{2}},$$

for all $\boldsymbol{\phi} \in \boldsymbol{V}(\mathcal{T}_h, \boldsymbol{k})$ with $1 \leq R_{\kappa_H} \leq \min(S_{\kappa_H}, K_{\kappa_H} + 1)$, $K_{\kappa_H} \geq 1$, for all $\kappa_H \in \mathcal{T}_H$, where C is a positive constant independent of $\boldsymbol{u}$, p, $\boldsymbol{h}$, $\boldsymbol{H}$, $\boldsymbol{k}$ and $\boldsymbol{K}$.

Proof. We write $A_{h,k}(\boldsymbol{u}_{H,K}; \boldsymbol{u}_{h,k}, \boldsymbol{\phi}) - A_{h,k}(\boldsymbol{u}_{h,k}; \boldsymbol{u}_{h,k}, \boldsymbol{\phi}) \equiv T_1 + T_2 + T_3$, where

$$T_1 = \int_\Omega (\mu(|\underline{e}_h(\boldsymbol{u}_{H,K})|) - \mu(|\underline{e}_h(\boldsymbol{u}_{h,k})|)) \underline{e}_h(\boldsymbol{u}_{h,k}) : \underline{e}_h(\boldsymbol{\phi}) \, d\boldsymbol{x},$$

$$T_2 = - \sum_{F \in \mathcal{F}_h} \int_F \{\!\!\{(\mu(|\underline{e}_h(\boldsymbol{u}_{H,K})|) - \mu(|\underline{e}_h(\boldsymbol{u}_{h,k})|)) \underline{e}_h(\boldsymbol{u}_{h,k})\}\!\!\} : [\![\boldsymbol{\phi}]\!] \, ds,$$

$$T_3 = \theta \sum_{F \in \mathcal{F}_h} \int_F \{\!\!\{(\mu(|h_F^{-1}[\![\boldsymbol{u}_{H,K}]\!]|) - \mu(h_F^{-1}|[\![\boldsymbol{u}_{h,k}]\!]|)) \underline{e}_h(\boldsymbol{\phi})\}\!\!\} : [\![\boldsymbol{u}_{h,k}]\!] \, ds.$$

Employing analogous arguments to those presented in the proof of Theorem 3.1 in [15], we get

$$|A_{h,k}(\boldsymbol{u}_{H,K}; \boldsymbol{u}_{h,k}, \boldsymbol{\phi}) - A_{h,k}(\boldsymbol{u}_{h,k}; \boldsymbol{u}_{h,k}, \boldsymbol{\phi})|$$
$$\leq C \left\{ \|\boldsymbol{u} - \boldsymbol{u}_{h,k}\|_{h,k} + \|\underline{e}_H(\boldsymbol{u} - \boldsymbol{u}_{H,K})\|_{L^2(\Omega)} \right\} \|\boldsymbol{\phi}\|_{h,k},$$

where C is a positive constant, independent of the discretization parameters. Since $\boldsymbol{V}(\mathcal{T}_H, \boldsymbol{K}) \subseteq \boldsymbol{V}(\mathcal{T}_h, \boldsymbol{k})$ and $Q(\mathcal{T}_H, \boldsymbol{K}) \subseteq Q(\mathcal{T}_h, \boldsymbol{k})$, applying Theorem 3 completes the proof. $\square$

We now proceed to prove Theorem 4. Writing $\boldsymbol{\phi} = \boldsymbol{u}_{h,k} - \boldsymbol{u}_{2G} \in \boldsymbol{V}(\mathcal{T}_h, \boldsymbol{k})$, by Lemma 2 we note that there exists a positive constant C, independent of h and $\boldsymbol{k}$, such that

$$C \|\boldsymbol{u}_{h,k} - \boldsymbol{u}_{2G}\|^2_{h,k} \leq A_{h,k}(\boldsymbol{u}_{H,K}; \boldsymbol{u}_{h,k} - \boldsymbol{u}_{2G}, \boldsymbol{\phi})$$
$$= A_{h,k}(\boldsymbol{u}_{H,K}; \boldsymbol{u}_{h,k}, \boldsymbol{\phi}) - A_{h,k}(\boldsymbol{u}_{H,K}; \boldsymbol{u}_{2G}, \boldsymbol{\phi}).$$

By subtracting (10) from (16) we note that $B_{h,k}(\boldsymbol{\phi}, q_{h,k}) = 0$ for all $q_{h,k} \in Q(\mathcal{T}_h, \boldsymbol{k})$. Hence, since $\boldsymbol{\phi} \in \boldsymbol{V}(\mathcal{T}_h, \boldsymbol{k})$ and $p_{2G}, p_{h,k} \in Q(\mathcal{T}_h, \boldsymbol{k})$, applying (15) and (9) gives

$$C \|\boldsymbol{u}_{h,k} - \boldsymbol{u}_{2G}\|^2_{h,k} \leq A_{h,k}(\boldsymbol{u}_{H,K}; \boldsymbol{u}_{h,k}, \boldsymbol{\phi}) - A_{h,k}(\boldsymbol{u}_{H,K}; \boldsymbol{u}_{2G}, \boldsymbol{\phi}) - B_{h,k}(\boldsymbol{\phi}, p_{2G})$$
$$= A_{h,k}(\boldsymbol{u}_{H,K}; \boldsymbol{u}_{h,k}, \boldsymbol{\phi}) - F_{h,k}(\boldsymbol{\phi})$$
$$= A_{h,k}(\boldsymbol{u}_{H,K}; \boldsymbol{u}_{h,k}, \boldsymbol{\phi}) - A_{h,k}(\boldsymbol{u}_{h,k}; \boldsymbol{u}_{h,k}, \boldsymbol{\phi}) - B_{h,k}(\boldsymbol{\phi}, p_{h,k})$$
$$= A_{h,k}(\boldsymbol{u}_{H,K}; \boldsymbol{u}_{h,k}, \boldsymbol{\phi}) - A_{h,k}(\boldsymbol{u}_{h,k}; \boldsymbol{u}_{h,k}, \boldsymbol{\phi}).$$

Application of Lemma 5 completes the proof of the first bound in Theorem 4.

We now consider the proof of the second bound in Theorem 4. From the inf-sup condition (12), there exists $\boldsymbol{\xi} \in \boldsymbol{V}(\mathcal{T}_h, \boldsymbol{k})$ such that

$$(20) \qquad \nu k_{\max}^{-1} \|p_{h,k} - p_{2G}\|_{L^2(\Omega)} \leq \frac{B_{h,k}(\boldsymbol{\xi}, p_{h,k} - p_{2G})}{\|\boldsymbol{\xi}\|_{h,k}}.$$

Subtracting (15) from (9) gives

$$B_{h,k}(\boldsymbol{\xi}, p_{h,k} - p_{2G}) = A_{h,k}(\boldsymbol{u}_{H,K}; \boldsymbol{u}_{2G}, \boldsymbol{\xi}) - A_{h,k}(\boldsymbol{u}_{h,k}; \boldsymbol{u}_{h,k}, \boldsymbol{\xi})$$
$$= A_{h,k}(\boldsymbol{u}_{H,K}; \boldsymbol{u}_{2G} - \boldsymbol{u}_{h,k}, \boldsymbol{\xi}) + A_{h,k}(\boldsymbol{u}_{H,K}; \boldsymbol{u}_{h,k}, \boldsymbol{\xi})$$
$$(21) \qquad\qquad - A_{h,k}(\boldsymbol{u}_{h,k}; \boldsymbol{u}_{h,k}, \boldsymbol{\xi}).$$

We note that the last two terms in (21) can be bounded based on employing Lemma 5. To bound the first term, we proceed as follows.

$$A_{h,k}(\boldsymbol{u}_{H,K}; \boldsymbol{u}_{2G} - \boldsymbol{u}_{h,k}, \boldsymbol{\xi})$$

$$\leq \int_{\Omega} |\mu(|\underline{e}_h(\boldsymbol{u}_{H,K})|)||\underline{e}_h(\boldsymbol{u}_{2G} - \boldsymbol{u}_{h,k})||\underline{e}_h(\boldsymbol{\xi})|\, \mathrm{d}\boldsymbol{x}$$

$$+ \sum_{F \in \mathcal{F}_h} \int_F \sigma_{h,k}|[\![\boldsymbol{u}_{2G} - \boldsymbol{u}_{h,k}]\!]||[\![\boldsymbol{\xi}]\!]|\, \mathrm{d}s$$

$$+ \sum_{F \in \mathcal{F}_h} \int_F \{\!\!\{|\mu(|\underline{e}_h(\boldsymbol{u}_{H,K})|)||\underline{e}_h(\boldsymbol{u}_{2G} - \boldsymbol{u}_{h,k})|\}\!\!\}|[\![\boldsymbol{\xi}]\!]|\, \mathrm{d}\boldsymbol{x}$$

$$+ |\theta| \sum_{F \in \mathcal{F}_h} \int_F \{\!\!\{|\mu(h_F^{-1}|[\![\boldsymbol{u}_{H,K}]\!]|)||\underline{e}_h(\boldsymbol{\xi})|\}\!\!\}|[\![\boldsymbol{u}_{2G} - \boldsymbol{u}_{h,k}]\!]|\, \mathrm{d}\boldsymbol{x}$$

$$\leq M_\mu \|\underline{e}_h(\boldsymbol{u}_{2G} - \boldsymbol{u}_{h,k})\|_{L^2(\Omega)} \|\underline{e}_h(\boldsymbol{\xi})\|_{L^2(\Omega)}$$

$$+ M_\mu C_T^{\frac{1}{2}} \gamma^{-\frac{1}{2}} \|\underline{e}_h(\boldsymbol{u}_{2G} - \boldsymbol{u}_{h,k})\|_{L^2(\Omega)} \left(\sum_{F \in \mathcal{F}_h} \sigma_{h,k} \left\| [\![\boldsymbol{\xi}]\!] \right\|_{L^2(F)}^2 \right)^{\frac{1}{2}}$$

$$+ M_\mu C_T^{\frac{1}{2}} \gamma^{-\frac{1}{2}} \|\underline{e}_h(\boldsymbol{\xi})\|_{L^2(\Omega)} \left(\sum_{F \in \mathcal{F}_h} \sigma_{h,k} \left\| [\![\boldsymbol{u}_{2G} - \boldsymbol{u}_{h,k}]\!] \right\|_{L^2(F)}^2 \right)^{\frac{1}{2}}$$

$$+ \left(\sum_{F \in \mathcal{F}_h} \sigma_{h,k} \left\| [\![\boldsymbol{u}_{2G} - \boldsymbol{u}_{h,k}]\!] \right\|_{L^2(F)}^2 \right)^{\frac{1}{2}} \left(\sum_{F \in \mathcal{F}_h} \sigma_{h,k} \left\| [\![\boldsymbol{\xi}]\!] \right\|_{L^2(F)}^2 \right)^{\frac{1}{2}}$$

$$\leq C \|\boldsymbol{u}_{h,k} - \boldsymbol{u}_{2G}\|_{h,k} \|\boldsymbol{\xi}\|_{h,k}.$$

Employing the first bound in Theorem 4 gives

$$A_{h,k}(\boldsymbol{u}_{H,K}; \boldsymbol{u}_{2G} - \boldsymbol{u}_{h,k}, \boldsymbol{\xi}) \leq C k_{\max}^2 \|\boldsymbol{\xi}\|_{h,k}$$

$$\times \left(\sum_{\kappa_H \in \mathcal{T}_H} \left\{ \frac{H_{\kappa_H}^{2R_{\kappa_H}-2}}{K_{\kappa_H}^{2S_{\kappa_H}-3}} \|\boldsymbol{u}\|_{H^{S_{\kappa_H}}(\kappa_H)}^2 + \frac{H_{\kappa_H}^{2R_{\kappa_H}-2}}{K_{\kappa_H}^{2S_{\kappa_H}-2}} \|p\|_{H^{S_{\kappa_H}-1}(\kappa_H)}^2 \right\} \right)^{\frac{1}{2}}.$$

Exploiting this result together with Lemma 5, equation (21) may be bounded by

$$B_{h,k}(\xi, p_{h,k} - p_{2G}) \leq C k_{\max}^2 \|\boldsymbol{\xi}\|_{h,k}$$

$$\times \left(\sum_{\kappa_H \in \mathcal{T}_H} \left\{ \frac{H_{\kappa_H}^{2R_{\kappa_H}-2}}{K_{\kappa_H}^{2S_{\kappa_H}-3}} \|\boldsymbol{u}\|_{H^{S_{\kappa_H}}(\kappa_H)}^2 + \frac{H_{\kappa_H}^{2R_{\kappa_H}-2}}{K_{\kappa_H}^{2S_{\kappa_H}-2}} \|p\|_{H^{S_{\kappa_H}-1}(\kappa_H)}^2 \right\} \right)^{\frac{1}{2}}.$$

Inserting this result into (20) and dividing through by $\nu k_{\max}^{-1}$ completes the proof of the second bound in Theorem 4. We note that an application of the triangle

inequality and Theorem 3 gives the bound in equation (19) and completes the proof. □.

3.2. A posteriori error bound. In this section we develop the *a posteriori* error analysis of the two-grid IP DGFEM defined by (13)–(16). Writing Π_{κ,k_κ} to denote the element-wise L^2-projection onto $\boldsymbol{V}(\mathcal{T}_h, \boldsymbol{k})$ we state the following upper bound.

Theorem 6. *Let* $(\boldsymbol{u}, p) \in H_0^1(\Omega)^d \times L_0^2(\Omega)$ *be the analytical solution of* (1)–(3), $(\boldsymbol{u}_{H,K}, p_{H,K}) \in \boldsymbol{V}(\mathcal{T}_H, \boldsymbol{K}) \times Q(\mathcal{T}_H, \boldsymbol{K})$ *the numerical approximation obtained from* (13)–(14) *and* $(\boldsymbol{u}_{2G}, p_{2G}) \in \boldsymbol{V}(\mathcal{T}_h, \boldsymbol{k}) \times Q(\mathcal{T}_h, \boldsymbol{k})$ *the numerical approximation obtained from* (15)–(16)*; then the following* hp-*a posteriori error bound holds*

$$\|(\boldsymbol{u} - \boldsymbol{u}_{2G}, p - p_{2G})\|_{\mathrm{DG}(h,k)}$$

$$\leq C \left(\sum_{\kappa \in \mathcal{T}_h} \left(\eta_\kappa^2 + \xi_\kappa^2 \right) + \sum_{\kappa \in \mathcal{T}_h} h_\kappa^2 k_\kappa^{-2} \|\boldsymbol{f} - \Pi_{\kappa,k_\kappa} \boldsymbol{f}\|_{L^2(\kappa)}^2 \right)^{\frac{1}{2}},$$

with a constant $C > 0$*, which is independent of* $\boldsymbol{h}$*,* $\boldsymbol{H}$*,* $\boldsymbol{k}$*,* $\boldsymbol{K}$*. Here, for all* $\kappa \in \mathcal{T}_h$*, the* local fine grid error indicators η_κ *are defined by*

(22)
$$\eta_\kappa^2 = h_\kappa^2 k_\kappa^{-2} \|\Pi_{\kappa,k_\kappa} \boldsymbol{f} + \nabla \cdot \{\mu(|\underline{e}(\boldsymbol{u}_{H,K})|)\underline{e}(\boldsymbol{u}_{2G})\}\|_{L^2(\kappa)}^2 + \|\nabla \cdot \boldsymbol{u}_{2G}\|_{L^2(\kappa)}^2$$

$$+ h_\kappa k_\kappa^{-1} \left\| [\![p_{2G}]\!] - \underline{[\![\mu(|\underline{e}(\boldsymbol{u}_{H,K})|)\underline{e}(\boldsymbol{u}_{2G})]\!]} \right\|_{L^2(\partial\kappa \setminus \Gamma)}^2 + \gamma^2 h_\kappa^{-1} k_\kappa^3 \left\| [\![\boldsymbol{u}_{2G}]\!] \right\|_{L^2(\partial\kappa)}^2$$

and the local two-grid error indicators ξ_κ *are defined, for all* $\kappa \in \mathcal{T}_h$*, by*

(23)
$$\xi_\kappa^2 = \|(\mu(|\underline{e}(\boldsymbol{u}_{H,K})|) - \mu(|\underline{e}(\boldsymbol{u}_{2G})|))\underline{e}(\boldsymbol{u}_{2G})\|_{L^2(\kappa)}^2.$$

3.2.1. Proof of Theorem 6. The proof of Theorem 6 follows as an extension of the corresponding *a posteriori* error bound for the standard hp-version IP DGFEM for strongly monotone quasi-Newtonian fluid flows, see [13] for details. We consider an auxiliary one-irregular fine mesh partition $\mathcal{T}_{\widetilde{h}}$ obtained from $\mathcal{T}_h$ by uniform subdivision of all elements $\kappa \in \mathcal{T}_h$ where an edge in κ contains a hanging node, cf. [35, Section 4.2] for the two-dimensional case and [34, Section 4.2] for three dimensions. We denote by $\boldsymbol{V}(\mathcal{T}_{\widetilde{h}}, \widetilde{\boldsymbol{k}})$ and $Q(\mathcal{T}_{\widetilde{h}}, \widetilde{\boldsymbol{k}})$ the corresponding DGFEM finite element spaces with polynomial degree vector $\widetilde{\boldsymbol{k}}$ defined by $\widetilde{k}_{\widetilde{\kappa}} = k_\kappa$, for any $\widetilde{\kappa} \in \mathcal{T}_{\widetilde{h}}$ with $\widetilde{\kappa} \subseteq \kappa$ and some $\kappa \in \mathcal{T}_h$. We note that $\boldsymbol{V}(\mathcal{T}_{\widetilde{h}}, \widetilde{\boldsymbol{k}}) \subseteq \boldsymbol{V}(\mathcal{T}_h, \boldsymbol{k})$, $Q(\mathcal{T}_{\widetilde{h}}, \widetilde{\boldsymbol{k}}) \subseteq Q(\mathcal{T}_h, \boldsymbol{k})$ and due to the assumptions in Section 2, the energy norms $\|\cdot\|_{h,k}$ and $\|\cdot\|_{\widetilde{h},\widetilde{k}}$ corresponding to the spaces $\boldsymbol{V}(\mathcal{T}_h, \boldsymbol{k})$ and $\boldsymbol{V}(\mathcal{T}_{\widetilde{h}}, \widetilde{\boldsymbol{k}})$, respectively, are equivalent on $\boldsymbol{V}(\mathcal{T}_h, \boldsymbol{k})$; in particular there exists positive constants c_1 and c_2, independent of the discretization parameters, such that

(24) $$c_1 \sum_{F \in \mathcal{F}_h} \int_F \sigma_{h,k} |[\![\boldsymbol{v}]\!]|^2 \, \mathrm{d}s \leq \sum_{\widetilde{F} \in \mathcal{F}_{\widetilde{h}}} \int_{\widetilde{F}} \sigma_{\widetilde{h},\widetilde{k}} |[\![\boldsymbol{v}]\!]|^2 \, \mathrm{d}s \leq c_2 \sum_{F \in \mathcal{F}_h} \int_F \sigma_{h,k} |[\![\boldsymbol{v}]\!]|^2 \, \mathrm{d}s$$

for all $\boldsymbol{v} \in \boldsymbol{V}(\mathcal{T}_h, \boldsymbol{k})$, cf. [13, 21, 35]. Here, $\mathcal{F}_{\widetilde{h}}$ denotes the set of all faces in the mesh $\mathcal{T}_{\widetilde{h}}$ and $\sigma_{\widetilde{h},\widetilde{k}}$ is the discontinuous penalization parameter on $\boldsymbol{V}(\mathcal{T}_{\widetilde{h}}, \widetilde{\boldsymbol{k}})$ which is defined analogously to $\sigma_{h,k}$ on $\boldsymbol{V}(\mathcal{T}_h, \boldsymbol{k})$.

Following the approach developed in the articles [22, 19], for example, we write

$$\boldsymbol{V}(\mathcal{T}_{\widetilde{h}}, \widetilde{\boldsymbol{k}}) = \left[\boldsymbol{V}(\mathcal{T}_{\widetilde{h}}, \widetilde{\boldsymbol{k}}) \right]^c \oplus_{\|\cdot\|_{\widetilde{h},\widetilde{k}}} \left[\boldsymbol{V}(\mathcal{T}_{\widetilde{h}}, \widetilde{\boldsymbol{k}}) \right]^\perp,$$

where $\left[\boldsymbol{V}(\mathcal{T}_{\widetilde{h}}, \widetilde{\boldsymbol{k}}) \right]^c = \boldsymbol{V}(\mathcal{T}_{\widetilde{h}}, \widetilde{\boldsymbol{k}}) \cap H_0^1(\Omega)^d$. Thereby, the solution $\boldsymbol{u}_{2G}$ obtained by (13)–(16) may be split accordingly

$$(25) \qquad\qquad \boldsymbol{u}_{2G} = \boldsymbol{u}_{2G}^c + \boldsymbol{u}_{2G}^\perp,$$

where $\boldsymbol{u}_{2G}^c \in \left[\boldsymbol{V}(\mathcal{T}_{\widetilde{h}}, \widetilde{\boldsymbol{k}}) \right]^c$ and $\boldsymbol{u}_{2G}^\perp \in \left[\boldsymbol{V}(\mathcal{T}_{\widetilde{h}}, \widetilde{\boldsymbol{k}}) \right]^\perp$. We can define the error in the velocity vector and pressure obtained by (13)–(16) as

$$(26) \qquad\qquad \boldsymbol{e_u} = \boldsymbol{u} - \boldsymbol{u}_{2G}, \qquad e_p = p - p_{2G},$$

respectively, and let

$$(27) \qquad\qquad \boldsymbol{e}_{\boldsymbol{u}}^c = \boldsymbol{u} - \boldsymbol{u}_{2G}^c \in H_0^1(\Omega)^d.$$

We now state the following auxiliary result.

Lemma 7. *With $\boldsymbol{u}_{2G}^\perp$ defined by (25), the following bound holds*

$$\left\| \boldsymbol{u}_{2G}^\perp \right\|_{\widetilde{h}, \widetilde{k}} \le C \left(\sum_{F \in \mathcal{F}_h} \int_F \sigma_{h,k} |[\![\boldsymbol{u}_{2G}]\!]|^2 \, \mathrm{d}s \right)^{\frac{1}{2}}$$

where the positive constant C is independent of γ and the discretization parameters, but depends only on the shape regularity of the mesh and the constants ρ_1 and ρ_2 from (7) and (8), respectively.

Proof. This proof follows in an analogous manner to the proof of [35, Lemma 4.6] and [34, Lemma 4.1], for the case when $d = 2, 3$, respectively. $\square$

In order to prove the *a posteriori* error bound stated in Theorem 6, we set

$$(28) \qquad \mathcal{A}_{h,k}(\boldsymbol{\psi}; \boldsymbol{u}, p, \boldsymbol{v}, q) = A_{h,k}(\boldsymbol{\psi}; \boldsymbol{u}, \boldsymbol{v}) + B_{h,k}(\boldsymbol{v}, p) - B_{h,k}(\boldsymbol{u}, q).$$

With this notation the following inf-sup stability result holds.

Lemma 8. *There exists a positive constant C_S, independent of the discretization parameters, such that for any $(\boldsymbol{u}, p) \in H_0^1(\Omega)^d \times L_0^2(\Omega)$ and $(\boldsymbol{w}, r) \in H_0^1(\Omega)^d \times L_0^2(\Omega)$, there exists $(\boldsymbol{v}, q) \in H_0^1(\Omega)^d \times L_0^2(\Omega)$ with*

$$\mathcal{A}_{h,k}(\boldsymbol{u}; \boldsymbol{u}, p, \boldsymbol{v}, q) - \mathcal{A}_{h,k}(\boldsymbol{w}; \boldsymbol{w}, r, \boldsymbol{v}, q) \ge C_S \left\| (\boldsymbol{u} - \boldsymbol{w}, p - r) \right\|_{\mathrm{DG}(h,k)},$$

$$\left\| (\boldsymbol{v}, q) \right\|_{\mathrm{DG}(h,k)} \le 1.$$

Proof. See [13, Proposition 2.4b]. $\square$

The proof of Theorem 6 now follows in a similar fashion as for the standard IP DGFEM for the numerical approximation of the non-Newtonian fluid flow problem (9)–(10), cf. [13]. Recalling the definition of the error, defined in (26), by (25), (24), Lemma 7 and the fact that $\gamma \ge 1$ and $k_\kappa \ge 1$, we have that

$$\left\| \boldsymbol{e_u}, e_p) \right\|_{\mathrm{DG}(h,k)} \le \left\| (\boldsymbol{e}_{\boldsymbol{u}}^c, e_p) \right\|_{\mathrm{DG}(h,k)} + \left\| \boldsymbol{u}_{2G}^\perp \right\|_{h,k}$$

$$(29) \qquad\qquad\qquad \le \left\| (\boldsymbol{e}_{\boldsymbol{u}}^c, e_p) \right\|_{\mathrm{DG}(h,k)} + C \left(\sum_{\kappa \in \mathcal{T}_h} \eta_\kappa^2 \right)^{\frac{1}{2}}.$$

Employing Lemma 8, we note that there exists $(\boldsymbol{v}, q) \in H_0^1(\Omega)^d \times L_0^2(\Omega)$ such that

$$C_S \left\| (\boldsymbol{e}_{\boldsymbol{u}}^c, e_p) \right\|_{\mathrm{DG}(h,k)} \le \mathcal{A}_{h,k}(\boldsymbol{u}; \boldsymbol{u}, p, \boldsymbol{v}, q) - \mathcal{A}_{h,k}(\boldsymbol{u}_{2G}^c; \boldsymbol{u}_{2G}^c, p_{2G}, \boldsymbol{v}, q),$$

$\|(\boldsymbol{v}, q)\|_{\mathrm{DG}(h,k)} \le 1$. Therefore, from (25), we deduce that

$$C_S \, \|(\boldsymbol{e}_{\boldsymbol{u}}^c, e_p)\|_{\mathrm{DG}(h,k)}$$

$$\le \sum_{\widetilde{\kappa} \in \mathcal{T}_{\widetilde{h}}} \int_{\widetilde{\kappa}} \{ \mu(|\underline{e}(\boldsymbol{u})|) \underline{e}(\boldsymbol{u}) - \mu(|\underline{e}(\boldsymbol{u}_{2G}^c)|) \underline{e}(\boldsymbol{u}_{2G}^c) \} : \underline{e}(\boldsymbol{v}) \, \mathrm{d}\boldsymbol{x}$$

$$- \sum_{\widetilde{\kappa} \in \mathcal{T}_{\widetilde{h}}} \int_{\widetilde{\kappa}} (p - p_{2G}) \nabla \cdot \boldsymbol{v} \, \mathrm{d}\boldsymbol{x} + \sum_{\widetilde{\kappa} \in \mathcal{T}_{\widetilde{h}}} \int_{\widetilde{\kappa}} q \nabla \cdot (\boldsymbol{u} - \boldsymbol{u}_{2G}^c) \, \mathrm{d}\boldsymbol{x}$$

$$= \sum_{\widetilde{\kappa} \in \mathcal{T}_{\widetilde{h}}} \int_{\widetilde{\kappa}} \{ \mu(|\underline{e}(\boldsymbol{u})|) \underline{e}(\boldsymbol{u}) - \mu(|\underline{e}(\boldsymbol{u}_{H,K})|) \underline{e}(\boldsymbol{u}_{2G}) \} : \underline{e}(\boldsymbol{v}) \, \mathrm{d}\boldsymbol{x}$$

$$+ \sum_{\widetilde{\kappa} \in \mathcal{T}_{\widetilde{h}}} \int_{\widetilde{\kappa}} \{ \mu(|\underline{e}(\boldsymbol{u}_{H,K})|) \underline{e}(\boldsymbol{u}_{2G}) - \mu(|\underline{e}(\boldsymbol{u}_{2G})|) \underline{e}(\boldsymbol{u}_{2G}) \} : \underline{e}(\boldsymbol{v}) \, \mathrm{d}\boldsymbol{x}$$

$$+ \sum_{\widetilde{\kappa} \in \mathcal{T}_{\widetilde{h}}} \int_{\widetilde{\kappa}} \{ \mu(|\underline{e}(\boldsymbol{u}_{2G})|) \underline{e}(\boldsymbol{u}_{2G}) - \mu(|\underline{e}(\boldsymbol{u}_{2G}^c)|) \underline{e}(\boldsymbol{u}_{2G}^c) \} : \underline{e}(\boldsymbol{v}) \, \mathrm{d}\boldsymbol{x}$$

$$- \sum_{\widetilde{\kappa} \in \mathcal{T}_{\widetilde{h}}} \int_{\widetilde{\kappa}} (p - p_{2G}) \nabla \cdot \boldsymbol{v} \, \mathrm{d}\boldsymbol{x} + \sum_{\widetilde{\kappa} \in \mathcal{T}_{\widetilde{h}}} \int_{\widetilde{\kappa}} q \nabla \cdot (\boldsymbol{u} - \boldsymbol{u}_{2G} + \boldsymbol{u}_{2G}^{\perp}) \, \mathrm{d}\boldsymbol{x}$$

$$(30) \qquad \equiv T_1 + T_2 + T_3,$$

where

$$T_1 = \sum_{\widetilde{\kappa} \in \mathcal{T}_{\widetilde{h}}} \int_{\widetilde{\kappa}} \{ \mu(|\underline{e}(\boldsymbol{u})|) \underline{e}(\boldsymbol{u}) - \mu(|\underline{e}(\boldsymbol{u}_{H,K})|) \underline{e}(\boldsymbol{u}_{2G}) \} : \underline{e}(\boldsymbol{v}) \, \mathrm{d}\boldsymbol{x}$$

$$- \sum_{\widetilde{\kappa} \in \mathcal{T}_{\widetilde{h}}} \int_{\widetilde{\kappa}} (p - p_{2G}) \nabla \cdot \boldsymbol{v} \, \mathrm{d}\boldsymbol{x} + \sum_{\widetilde{\kappa} \in \mathcal{T}_{\widetilde{h}}} \int_{\widetilde{\kappa}} q \nabla \cdot (\boldsymbol{u} - \boldsymbol{u}_{2G}) \, \mathrm{d}\boldsymbol{x},$$

$$T_2 = \sum_{\widetilde{\kappa} \in \mathcal{T}_{\widetilde{h}}} \int_{\widetilde{\kappa}} \{ \mu(|\underline{e}(\boldsymbol{u}_{2G})|) \underline{e}(\boldsymbol{u}_{2G}) - \mu(|\underline{e}(\boldsymbol{u}_{2G}^c)|) \underline{e}(\boldsymbol{u}_{2G}^c) \} : \underline{e}(\boldsymbol{v}) \, \mathrm{d}\boldsymbol{x}$$

$$+ \sum_{\widetilde{\kappa} \in \mathcal{T}_{\widetilde{h}}} \int_{\widetilde{\kappa}} q \nabla \cdot \boldsymbol{u}_{2G}^{\perp} \, \mathrm{d}\boldsymbol{x},$$

$$T_3 = \sum_{\widetilde{\kappa} \in \mathcal{T}_{\widetilde{h}}} \int_{\widetilde{\kappa}} \{ \mu(|\underline{e}(\boldsymbol{u}_{H,K})|) \underline{e}(\boldsymbol{u}_{2G}) - \mu(|\underline{e}(\boldsymbol{u}_{2G})|) \underline{e}(\boldsymbol{u}_{2G}) \} : \underline{e}(\boldsymbol{v}) \, \mathrm{d}\boldsymbol{x}.$$

We note that T_1 and T_2 are analogous to the corresponding terms that arise in the *a posteriori* error analysis of the standard IP DGFEM discretization of (1)–(3), cf. [13]. Indeed, by following the analysis presented in [13], we deduce that

$$(31) \qquad |T_1| + |T_2| \le C \left(\sum_{\kappa \in \mathcal{T}_h} \eta_\kappa^2 + \sum_{\kappa \in \mathcal{T}_h} h_\kappa^2 k_\kappa^{-2} \, \|\boldsymbol{f} - \Pi_{\kappa, k_\kappa} \boldsymbol{f}\|_{L^2(\kappa)}^2 \right)^{\frac{1}{2}}.$$

We note that term T_3 may be bounded in a similar manner to the corresponding term which arises in the two-grid IP DGFEM of the second-order quasilinear scalar

elliptic problem, cf. [15]; indeed, we have

$$|T_3| \leq \sum_{\kappa \in \mathcal{T}_h} \int_{\widetilde{\kappa}} |\mu(|\underline{e}(\boldsymbol{u}_{H,K})|)\underline{e}(\boldsymbol{u}_{2G}) - \mu(|\underline{e}(\boldsymbol{u}_{2G})|)\underline{e}(\boldsymbol{u}_{2G})||\underline{e}(\boldsymbol{v})| \, \mathrm{d}\boldsymbol{x}$$

$$\leq \left(\sum_{\kappa \in \mathcal{T}_h} \|\{\mu(|\underline{e}(\boldsymbol{u}_{H,K})|) - \mu(|\underline{e}(\boldsymbol{u}_{2G})|)\}\underline{e}(\boldsymbol{u}_{2G})\|_{L^2(\kappa)}^2 \right)^{\frac{1}{2}} \left(\sum_{\kappa \in \mathcal{T}_h} \|\underline{e}(\boldsymbol{v})\|_{L^2(\kappa)}^2 \right)^{\frac{1}{2}}$$

$$\leq \left(\sum_{\kappa \in \mathcal{T}_h} \xi_\kappa^2 \right)^{\frac{1}{2}} \|(\boldsymbol{v}, q)\|_{\mathrm{DG}(h,k)}$$

(32)

$$\leq \left(\sum_{\kappa \in \mathcal{T}_h} \xi_\kappa^2 \right)^{\frac{1}{2}}.$$

Inserting (31) and (32) into (30) gives

$$\|(\boldsymbol{e}_{\boldsymbol{u}}^c, e_p)\|_{\mathrm{DG}(h,k)} \leq C_S^{-1} C \left(\sum_{\kappa \in \mathcal{T}_h} \eta_\kappa^2 + \sum_{\kappa \in \mathcal{T}_h} h_\kappa^2 k_\kappa^{-2} \|\boldsymbol{f} - \Pi_{\kappa,k_\kappa} \boldsymbol{f}\|_{L^2(\kappa)}^2 \right)^{\frac{1}{2}}$$

$$+ C_S^{-1} \left(\sum_{\kappa \in \mathcal{T}_h} \xi_\kappa^2 \right)^{\frac{1}{2}}.$$

Combining this result with (29) and applying the Cauchy inequality completes the proof of Theorem 6. $\qquad\square$

Remark 1. For brevity we omit lower error bounds for the numerical approximation $(\boldsymbol{u}_{2G}, p_{2G})$ obtained from (13)–(16) as the proof follows in an analogous manner to the analysis presented in [15] and [13]; for details, see [11].

4. Two-grid hp-Version IP DGFEM based on an Incomplete Newton iteration

In this section we turn our attention to a family of two-grid IP DGFEMs for the numerical approximation of (1)–(3) based on employing a single step of a Newton iteration on the fine finite element space, cf. [5, 12, 33]. Using the same notation defined in the previous section, the two-grid version of the IP DGFEM discretization of (1)–(3) is defined by:

(1) (Nonlinear solve) Compute $(\boldsymbol{u}_{H,K}, p_{H,K}) \in \boldsymbol{V}(\mathcal{T}_H, \boldsymbol{K}) \times Q(\mathcal{T}_H, \boldsymbol{K})$ such that

(33) $\qquad A_{H,K}(\boldsymbol{u}_{H,K}; \boldsymbol{u}_{H,K}, \boldsymbol{v}_{H,K}) + B_{H,K}(\boldsymbol{v}_{H,K}, p_{H,K}) = F_{H,K}(\boldsymbol{v}_{H,K}),$

(34) $\qquad\qquad\qquad\qquad -B_{H,K}(\boldsymbol{u}_{H,K}, q_{H,K}) = 0$

for all $(\boldsymbol{v}_{H,K}, q_{H,K}) \in \boldsymbol{V}(\mathcal{T}_H, \boldsymbol{K}) \times Q(\mathcal{T}_H, \boldsymbol{K})$.

(2) (Linear solve) Determine the fine grid solution $(\boldsymbol{u}_{2G}, p_{2G}) \in \boldsymbol{V}(\mathcal{T}_h, \boldsymbol{k}) \times Q(\mathcal{T}_h, \boldsymbol{k})$ such that

$A'_{h,k}[\boldsymbol{u}_{H,K}](\boldsymbol{u}_{2G}, \boldsymbol{v}_{h,k}) + B_{h,k}(\boldsymbol{v}_{h,k}, p_{2G}) = A'_{h,k}[\boldsymbol{u}_{H,K}](\boldsymbol{u}_{H,K}, \boldsymbol{v}_{h,k})$

(35) $\qquad\qquad\qquad\qquad - A_{h,k}(\boldsymbol{u}_{H,K}; \boldsymbol{u}_{H,K}, \boldsymbol{v}_{h,k}) + F_{h,k}(\boldsymbol{v}_{h,k}),$

(36) $\qquad\qquad -B_{h,k}(\boldsymbol{u}_{2G}, q_{h,k}) = 0$

for all $(\boldsymbol{v}_{h,k}, q_{h,k}) \in \boldsymbol{V}(\mathcal{T}_h, \boldsymbol{k}) \times Q(\mathcal{T}_h, \boldsymbol{k})$.

Here $A'_{h,k}[\boldsymbol{u}](\boldsymbol{\phi}, \boldsymbol{v})$ denotes the Fréchet derivative of $\boldsymbol{u} \to A_{h,k}(\boldsymbol{u}; \boldsymbol{u}, \boldsymbol{v})$, for fixed $\boldsymbol{v}$, evaluated at $\boldsymbol{u}$; thereby, given $\boldsymbol{\phi}$ we have

$$A'_{h,k}[\boldsymbol{u}](\boldsymbol{\phi}, \boldsymbol{v}) = \lim_{t \to 0} \frac{A_{h,k}(\boldsymbol{u} + t\boldsymbol{\phi}; \boldsymbol{u} + t\boldsymbol{\phi}, \boldsymbol{v}) - A_{h,k}(\boldsymbol{u}; \boldsymbol{u}, \boldsymbol{v})}{t}.$$

For simplicity of presentation, in this section we only consider the incomplete IP DGFEM formulation corresponding to the case when $\theta = 0$. In addition, we strengthen the regularity assumption on the nonlinearity μ, cf. Assumption 1, as follows.

Assumption 2. We assume that the stricter regularity condition $\mu \in \mathrm{C}^2(\bar{\Omega} \times [0, \infty))$ holds.

For the proceeding error analysis we state the following inf-sup stability result.

Lemma 9. *For any* $(\boldsymbol{u}, p) \in \boldsymbol{V}(\mathcal{T}_h, \boldsymbol{k}) \times Q(\mathcal{T}_h, \boldsymbol{k})$ *and* $\boldsymbol{w} \in \boldsymbol{V}(\mathcal{T}_h, \boldsymbol{k})$, *there exists* $(\boldsymbol{v}, q) \in \boldsymbol{V}(\mathcal{T}_h, \boldsymbol{k}) \times Q(\mathcal{T}_h, \boldsymbol{k})$ *such that*

$$C_S k_{max}^{-2} \|(\boldsymbol{u}, p)\|_{\mathrm{DG}(h,k)} \le A'_{h,k}[\boldsymbol{w}](\boldsymbol{u}, \boldsymbol{v}) + B_{h,k}(\boldsymbol{v}, p) - B_{h,k}(\boldsymbol{u}, q),$$
$$\|(\boldsymbol{v}, q)\|_{\mathrm{DG}(h,k)} \le 1,$$

where C_S *is a positive constant, independent of the discretization parameters.*

Proof. From [13, Proposition 3.2(b)], the following inf-sup stability bound holds: for any $(\boldsymbol{w}_1, r_1), (\boldsymbol{w}_2, r_2) \in \boldsymbol{V}(\mathcal{T}_h, \boldsymbol{k}) \times Q(\mathcal{T}_h, \boldsymbol{k})$ there exists $(\boldsymbol{v}, q) \in \boldsymbol{V}(\mathcal{T}_h, \boldsymbol{k}) \times Q(\mathcal{T}_h, \boldsymbol{k})$ such that

$$C_S k_{max}^{-2} \|(\boldsymbol{w}_1 - \boldsymbol{w}_2, r_1 - r_2)\|_{\mathrm{DG}(h,k)} \le A_{h,k}(\boldsymbol{w}_1; \boldsymbol{w}_1, \boldsymbol{v}) - A_{h,k}(\boldsymbol{w}_2; \boldsymbol{w}_2, \boldsymbol{v})$$
$$+ B_{h,k}(\boldsymbol{v}, r_1 - r_2) - B_{h,k}(\boldsymbol{w}_1 - \boldsymbol{w}_2, q),$$
$$\|(\boldsymbol{v}, q)\|_{\mathrm{DG}(h,k)} \le 1.$$

By setting $\boldsymbol{w}_1 = \boldsymbol{w} + t\boldsymbol{u}$, $\boldsymbol{w}_2 = \boldsymbol{w}$, $r_1 = tp$ and $r_2 = 0$, where $t > 0$ then

$$C_S k_{max}^{-2} \|(t\boldsymbol{u}, tp)\|_{\mathrm{DG}(h,k)}$$
$$\le A_{h,k}(\boldsymbol{w} + t\boldsymbol{u}; \boldsymbol{w} + t\boldsymbol{u}, \boldsymbol{v}) - A_{h,k}(\boldsymbol{w}; \boldsymbol{w}, \boldsymbol{v}) + B_{h,k}(\boldsymbol{v}, tp) - B_{h,k}(t\boldsymbol{u}, q).$$

Thereby,

$$C_S k_{max}^{-2} \|(\boldsymbol{u}, p)\|_{\mathrm{DG}(h,k)} \le \frac{A_{h,k}(\boldsymbol{w} + t\boldsymbol{u}; \boldsymbol{w} + t\boldsymbol{u}, \boldsymbol{v}) - A_{h,k}(\boldsymbol{w}; \boldsymbol{w}, \boldsymbol{v})}{t}$$
$$+ B_{h,k}(\boldsymbol{v}, p) - B_{h,k}(\boldsymbol{u}, q).$$

Taking the limit as $t \to 0$ completes the proof. $\square$

4.1. A priori error bound. In this section we derive an *a priori* error bound for the two-grid approximation defined in (33)–(36) for the numerical approximation of the non-Newtonian fluid flow problem (1)–(3). For simplicity of presentation, in this section we assume that the mesh is quasi-uniform with (global) mesh size h; moreover, we assume that the polynomial degree is uniform over the mesh, and write k in lieu of $\boldsymbol{k}$.

Theorem 10. *Assuming that* $(\boldsymbol{u}, p) \in (C^1(\Omega) \cap H^s(\Omega))^d \times (C^1(\Omega) \cap H^{s-1}(\Omega))$, $s \geq 2$; *then the solution* $(\boldsymbol{u}_{2G}, p_{2G}) \in \boldsymbol{V}(\mathcal{T}_h, \boldsymbol{k}) \times Q(\mathcal{T}_h, \boldsymbol{k})$ *of the incomplete Newton two-grid method* (33)–(36) *satisfies the error bounds*

$$\|(\boldsymbol{u}_{h,k} - \boldsymbol{u}_{2G}, p_{h,k} - p_{2G})\|_{\mathrm{DG}(h,k)}$$

$$(37) \qquad \leq C \frac{k^{23/2}}{h} \left\{ \frac{H^{2R-2}}{K^{2s-3}} \|\boldsymbol{u}\|^2_{H^s(\Omega)} + \frac{H^{2R-2}}{K^{2s-2}} \|p\|^2_{H^{s-1}(\Omega)} \right\},$$

$$\|(\boldsymbol{u} - \boldsymbol{u}_{2G}, p - p_{h,k})\|_{\mathrm{DG}(h,k)}$$

$$\leq C k^2 \left\{ \frac{h^{2r-2}}{k^{2s-3}} \|\boldsymbol{u}\|^2_{H^s(\Omega)} + \frac{h^{2r-2}}{k^{2s-2}} \|p\|^2_{H^{s-1}(\Omega)} \right\}^{\frac{1}{2}}$$

$$(38) \qquad + C \frac{k^{23/2}}{h} \left\{ \frac{H^{2R-2}}{K^{2s-3}} \|\boldsymbol{u}\|^2_{H^s(\Omega)} + \frac{H^{2R-2}}{K^{2s-2}} \|p\|^2_{H^{s-1}(\Omega)} \right\},$$

with $1 \leq r \leq \min(s, k+1)$, $k \geq 1$ *and* $1 \leq R \leq \min(s, K+1)$, $K \geq 1$, *where* C *is a positive constant, independent of* $\boldsymbol{u}, p, h, H, k$ *and* K.

Remark 2. Theorem 10 represents the generalization of the corresponding bound derived in [12] for a scalar quasilinear PDE to the case of the non-Newtonian fluid flow problem defined in (33)–(36).

Remark 3. We note that the error bounds stated in Theorem 10 contain terms which have a strong dependence on the fine mesh polynomial degree k compared to the corresponding results derived for the two-grid IP DGFEM approximation of a scalar quasilinear elliptic PDE, cf. [12]; indeed, in this latter case the exponent of k is reduced from $23/2$ to $7/2$. This degradation in the suboptimal exponent of k is attributed to employing the discrete inf-sup condition (12) within the analysis, since this stability result depends on the maximum polynomial degree $k_{\max}$. It is worth remarking that [24, Remark 6.5] notes that numerical experiments undertaken for the Stokes equations in two dimensions, cf. [26], indicates that the discrete inf-sup condition is *independent* of the polynomial degree k and hence (12) may not be sharp with respect to k.

4.1.1. Auxiliary Results. In order to prove Theorem 10 we first state and prove the following auxiliary results.

Lemma 11. *For a function* $q \in Q(\mathcal{T}_h, \boldsymbol{k})$ *and a function* $\boldsymbol{v} \in \boldsymbol{V}(\mathcal{T}_h, \boldsymbol{k})$ *we have the inverse inequalities*

$$\|q\|_{L^4(\Omega)} \leq C k h^{-1/2} \|q\|_{L^2(\Omega)}, \qquad \|\boldsymbol{v}\|_{L^4(\Omega)} \leq C k h^{-1/2} \|\boldsymbol{v}\|_{L^2(\Omega)},$$

where C *is a positive constant, independent of the discretization parameters.*

Proof. See [12, Lemma 3.2] for details. □

Lemma 12. *For any* $\boldsymbol{v}, \boldsymbol{w}, \boldsymbol{\phi} \in \boldsymbol{V}(\mathcal{T}_h, \boldsymbol{k})$,

$$(39) \qquad A_{h,k}(\boldsymbol{w}; \boldsymbol{w}, \boldsymbol{\phi}) = A_{h,k}(\boldsymbol{v}; \boldsymbol{v}, \boldsymbol{\phi}) + A'_{h,k}[\boldsymbol{v}](\boldsymbol{w} - \boldsymbol{v}, \boldsymbol{\phi}) + \mathcal{Q}(\boldsymbol{v}, \boldsymbol{w}, \boldsymbol{\phi}),$$

where the remainder $\mathcal{Q}$ *satisfies*

$$|\mathcal{Q}(\boldsymbol{v}, \boldsymbol{w}, \boldsymbol{\phi})| \leq C k^2 h^{-1} \left(1 + \|\underline{e}(\boldsymbol{v})\|_{L^\infty(\Omega)} + \|\underline{e}(\boldsymbol{w})\|_{L^\infty(\Omega)} \right) \|\boldsymbol{w} - \boldsymbol{v}\|^2_{h,k} \|\boldsymbol{\phi}\|_{h,k},$$

where C *is a positive constant, independent of the discretization parameters.*

Proof. We follow the proof outlined by [33, Lemma 3.1], cf., also, [12]. To this end, setting $\boldsymbol{\xi}(t) = \boldsymbol{v} + t(\boldsymbol{w} - \boldsymbol{v})$ and $\eta(t) = A_{h,k}(\boldsymbol{\xi}(t); \boldsymbol{\xi}(t), \boldsymbol{\phi})$, we note that the first equation follows from the identity

$$\eta(1) = \eta(0) + \eta'(0) + \int_0^1 \eta''(t)(1-t)\,\mathrm{d}t$$

with

$$\mathcal{Q}(\boldsymbol{v}, \boldsymbol{w}, \boldsymbol{\xi}) = \int_0^1 \eta''(t)(1-t)\,\mathrm{d}t.$$

In particular,

$$\eta''(t) = A_{h,k}''[\boldsymbol{\xi}(t)](\boldsymbol{w} - \boldsymbol{v}, \boldsymbol{w} - \boldsymbol{v}, \boldsymbol{\phi});$$

thereby,

$$\begin{aligned}
\mathcal{Q}&(\boldsymbol{v}, \boldsymbol{w}, \boldsymbol{\phi})\\
&= 2\int_0^1 \int_\Omega \mu'_{\underline{e}(\boldsymbol{u})}(|\underline{e}(\boldsymbol{\xi}(t))|) : \underline{e}(\boldsymbol{w} - \boldsymbol{v})\underline{e}(\boldsymbol{w} - \boldsymbol{v}) : \underline{e}(\boldsymbol{\phi})\,\mathrm{d}\boldsymbol{x}(1-t)\,\mathrm{d}t\\
&\quad + \int_0^1 \int_\Omega \mu''_{\underline{e}(\boldsymbol{u})}(|\underline{e}(\boldsymbol{\xi}(t))|)|\underline{e}(\boldsymbol{w} - \boldsymbol{v})|^2 \underline{e}(\boldsymbol{\xi}(t)) : \underline{e}(\boldsymbol{\phi})\,\mathrm{d}\boldsymbol{x}(1-t)\,\mathrm{d}t\\
&\quad - 2\int_0^1 \sum_{F \in \mathcal{F}_h} \int_F \{\!\!\{\mu'_{\underline{e}(\boldsymbol{u})}(|\underline{e}(\boldsymbol{\xi}(t))|) : \underline{e}(\boldsymbol{w} - \boldsymbol{v})\underline{e}(\boldsymbol{w} - \boldsymbol{v})\}\!\!\} : [\![\boldsymbol{\phi}]\!]\,\mathrm{d}s(1-t)\,\mathrm{d}t\\
&\quad - \int_0^1 \sum_{F \in \mathcal{F}_h} \int_F \{\!\!\{\mu''_{\underline{e}(\boldsymbol{u})}(|\underline{e}(\boldsymbol{\xi}(t))|)|\underline{e}(\boldsymbol{w} - \boldsymbol{v})|^2 \underline{e}(\boldsymbol{\xi}(t))\}\!\!\} : [\![\boldsymbol{\phi}]\!]\,\mathrm{d}s(1-t)\,\mathrm{d}t\\
&\equiv T_1 + T_2 + T_3 + T_4.
\end{aligned}$$

Here, $\mu'_{\underline{e}(\boldsymbol{u})}(|\cdot|)$ and $\mu''_{\underline{e}(\boldsymbol{u})}(|\cdot|)$ denote the first and second derivatives of $\mu(|\cdot|)$, respectively. First consider T_1: employing Assumption 2 and Lemma 11 gives

$$T_1 \leq C\,\|\underline{e}(\boldsymbol{w} - \boldsymbol{v})\|_{L^4(\Omega)}^2\,\|\underline{e}(\boldsymbol{\phi})\|_{L^2(\Omega)} \leq Ck^2 h^{-1}\,\|\underline{e}(\boldsymbol{w} - \boldsymbol{v})\|_{L^2(\Omega)}^2\,\|\underline{e}(\boldsymbol{\phi})\|_{L^2(\Omega)}.$$

Secondly, term T_2 is bounded in an analogous manner as follows:

$$\begin{aligned}
T_2 &\leq C\left(\|\underline{e}(\boldsymbol{w})\|_{L^\infty(\Omega)} + \|\underline{e}(\boldsymbol{v})\|_{L^\infty(\Omega)}\right)\|\underline{e}(\boldsymbol{w} - \boldsymbol{v})\|_{L^4(\Omega)}^2\,\|\underline{e}(\boldsymbol{\phi})\|_{L^2(\Omega)}\\
&\leq C\left(\|\underline{e}(\boldsymbol{w})\|_{L^\infty(\Omega)} + \|\underline{e}(\boldsymbol{v})\|_{L^\infty(\Omega)}\right)k^2 h^{-1}\,\|\underline{e}(\boldsymbol{w} - \boldsymbol{v})\|_{L^2(\Omega)}^2\,\|\underline{e}(\boldsymbol{\phi})\|_{L^2(\Omega)}.
\end{aligned}$$

To bound Term T_3, we employ the inverse inequality stated in Lemma 1, together with Lemma 11; thereby, we get

$$\begin{aligned}
T_3 &\leq C\left\{\sum_{F \in \mathcal{F}_h} hk^{-2}\left\|\{\!\!\{|\underline{e}(\boldsymbol{w} - \boldsymbol{v})|^2\}\!\!\}\right\|_{L^2(F)}^2\right\}^{\frac{1}{2}}\left\{\sum_{F \in \mathcal{F}_h} \int_F k^2 h^{-1}|[\![\boldsymbol{\phi}]\!]|^2\,\mathrm{d}s\right\}^{\frac{1}{2}}\\
&\leq C\,\|\underline{e}(\boldsymbol{w} - \boldsymbol{v})\|_{L^4(\Omega)}^2\,\|\boldsymbol{\phi}\|_{h,p}\\
&\leq Ck^2 h^{-1}\,\|\underline{e}(\boldsymbol{w} - \boldsymbol{v})\|_{L^2(\Omega)}^2\,\|\boldsymbol{\phi}\|_{h,p}.
\end{aligned}$$

We can bound T_4 in an analogous fashion as follows:

$$T_4 \leq C \left\{ \sum_{F \in \mathcal{F}_h} h k^{-2} \left\| \{\!\!\{ |\underline{e}(\boldsymbol{w} - \boldsymbol{v})|^2 |\underline{e}(\boldsymbol{w})| \}\!\!\} \right\|_{L^2(F)}^2 \right\}^{\frac{1}{2}} \left\{ \sum_{F \in \mathcal{F}_h} \int_F k^2 h^{-1} |[\![\boldsymbol{\phi}]\!]|^2 \, \mathrm{d}s \right\}^{\frac{1}{2}}$$

$$+ C \left\{ \sum_{F \in \mathcal{F}_h} h k^{-2} \left\| \{\!\!\{ |\underline{e}(\boldsymbol{w} - \boldsymbol{v})|^2 |\underline{e}(\boldsymbol{v})| \}\!\!\} \right\|_{L^2(F)}^2 \right\}^{\frac{1}{2}} \left\{ \sum_{F \in \mathcal{F}_h} \int_F k^2 h^{-1} |[\![\boldsymbol{\phi}]\!]|^2 \, \mathrm{d}s \right\}^{\frac{1}{2}}$$

$$\leq C \left\{ \left\| |\underline{e}(\boldsymbol{w} - \boldsymbol{v})|^2 |\underline{e}(\boldsymbol{w})| \right\|_{L^2(\Omega)} + \left\| |\underline{e}(\boldsymbol{w} - \boldsymbol{v})|^2 |\underline{e}(\boldsymbol{w})| \right\|_{L^2(\Omega)} \right\} \|\boldsymbol{\phi}\|_{h,k}$$

$$\leq C \left\{ \|\underline{e}(\boldsymbol{w})\|_{L^\infty(\Omega)} + \|\underline{e}(\boldsymbol{v})\|_{L^\infty(\Omega)} \right\} \|\underline{e}(\boldsymbol{w} - \boldsymbol{v})\|_{L^4(\Omega)}^2 \|\boldsymbol{\phi}\|_{h,k}$$

$$\leq C k^2 h^{-1} \left\{ \|\underline{e}(\boldsymbol{w})\|_{L^\infty(\Omega)} + \|\underline{e}(\boldsymbol{v})\|_{L^\infty(\Omega)} \right\} \|\underline{e}(\boldsymbol{w} - \boldsymbol{v})\|_{L^2(\Omega)}^2 \|\boldsymbol{\phi}\|_{h,k} .$$

Combining these bounds for terms T_1, T_2, T_3 and T_4 completes the proof. $\qquad\square$

Lemma 13. *Let $(\boldsymbol{u}, p) \in H^2(\Omega)^d \times H^1(\Omega)$ be the analytical solution of (1)–(3) and $\boldsymbol{u}_{h,k} \in \boldsymbol{V}(\mathcal{T}_h, \boldsymbol{k})$ be the velocity component of the numerical solution defined by (9)–(10). Then, assuming that $\underline{e}(\boldsymbol{u}) \in L^\infty(\Omega)^{d \times d}$, we have that*

$$\|\underline{e}(\boldsymbol{u}_{h,k})\|_{L^\infty(\Omega)} \leq C k^{7/2},$$

where C is a positive constant, independent of the discretization parameters.

Proof. Writing $\mathcal{P}_{\boldsymbol{u}}$ to denote the projection of $\boldsymbol{u}$ onto the finite element space $\boldsymbol{V}(\mathcal{T}_h, \boldsymbol{k})$ defined in [6], we have that

$$\|\boldsymbol{u} - \mathcal{P}_{\boldsymbol{u}}\|_{H^q(\Omega)} \leq C \frac{h^{2-q}}{k^{2-q}} \|\boldsymbol{u}\|_{H^2(\Omega)}, \qquad \|\nabla(\boldsymbol{u} - \mathcal{P}_{\boldsymbol{u}})\|_{L^\infty(\Omega)} \leq C \|\boldsymbol{u}\|_{H^2(\Omega)}$$

for all $q \leq 2$. We also note the inequality

$$\|\underline{e}(\boldsymbol{v})\|_{L^\infty(\Omega)} = \left\| \tfrac{1}{2} \left(\nabla \boldsymbol{v} + (\nabla \boldsymbol{v})^\top \right) \right\|_{L^\infty(\Omega)}$$
$$\leq \tfrac{1}{2} \|\nabla \boldsymbol{v}\|_{L^\infty(\Omega)} + \tfrac{1}{2} \left\| (\nabla \boldsymbol{v})^\top \right\|_{L^\infty(\Omega)} = \|\nabla \boldsymbol{v}\|_{L^\infty(\Omega)} .$$

Exploiting these results, standard inverse inequalities, cf. [25], and Theorem 3, we get

$$\|\underline{e}(\boldsymbol{u}_{h,k})\|_{L^\infty(\Omega)} \leq \|\underline{e}(\boldsymbol{u}_{h,k} - \mathcal{P}_{\boldsymbol{u}})\|_{L^\infty(\Omega)} + \|\underline{e}(\mathcal{P}_{\boldsymbol{u}})\|_{L^\infty(\Omega)}$$
$$\leq C k^2 h^{-1} \|\underline{e}(\boldsymbol{u}_{h,k} - \mathcal{P}_{\boldsymbol{u}})\|_{L^2(\Omega)} + \|\underline{e}(\boldsymbol{u} - \mathcal{P}_{\boldsymbol{u}})\|_{L^\infty(\Omega)}$$
$$+ \|\underline{e}(\boldsymbol{u})\|_{L^\infty(\Omega)}$$
$$\leq C \left\{ k^2 h^{-1} \left(\|\boldsymbol{u} - \boldsymbol{u}_{h,k}\|_{h,k} + \|\underline{e}(\boldsymbol{u} - \mathcal{P}_{\boldsymbol{u}})\|_{L^2(\Omega)} \right) + \|\boldsymbol{u}\|_{H^2(\Omega)} \right\}$$
$$+ \|\underline{e}(\boldsymbol{u})\|_{L^\infty(\Omega)}$$
$$\leq C \left\{ \frac{k^4}{h} \left[\frac{h^2}{k} \|\boldsymbol{u}\|_{H^2(\Omega)}^2 + \frac{h^2}{k^2} \|p\|_{H^1(\Omega)}^2 \right]^{\frac{1}{2}} + (1+k) \|\boldsymbol{u}\|_{H^2(\Omega)} \right\}$$
$$+ \|\underline{e}(\boldsymbol{u})\|_{L^\infty(\Omega)}$$
$$\leq C k^{7/2} \left\{ \|\boldsymbol{u}\|_{H^2(\Omega)} + \|p\|_{H^1(\Omega)} + \|\underline{e}(\boldsymbol{u})\|_{L^\infty(\Omega)} \right\} .$$

Since $\boldsymbol{u} \in H^2(\Omega)^d$, $\underline{e}(\boldsymbol{u}) \in L^\infty(\Omega)^{d \times d}$, and $p \in H^1(\Omega)$, the quantities $\|\boldsymbol{u}\|_{H^2(\Omega)}$, $\|\underline{e}(\boldsymbol{u})\|_{L^\infty(\Omega)}$ and $\|p\|_{H^1(\Omega)}$ are bounded uniformly by a constant; this then completes the proof. $\qquad\square$

4.1.2. Proof of Theorem 10. We now employ the above results to prove Theorem 10. To this end, we define $\boldsymbol{\delta_u} = \boldsymbol{u}_{h,k} - \boldsymbol{u}_{2G}$ and $\delta_p = p_{h,k} - p_{2G}$. Then, from Lemma 9, there exists $(\boldsymbol{v}, q) \in \boldsymbol{V}(\mathcal{T}_h, \boldsymbol{k}) \times Q(\mathcal{T}_h, \boldsymbol{k})$ such that

$$(40) \quad C_S k^{-2} \|(\boldsymbol{\delta_u}, \delta_p)\|_{\mathrm{DG}(h,k)} \leq A'_{h,k}[\boldsymbol{u}_{H,K}](\boldsymbol{\delta_u}, \boldsymbol{v}) + B_{h,k}(\boldsymbol{v}, \delta_p) - B_{h,k}(\boldsymbol{\delta_u}, q),$$

$$(41) \quad \|(\boldsymbol{v}, q)\|_{\mathrm{DG}(h,k)} \leq 1.$$

Thereby, from (9), (10), (35), (36), and Lemma 12 we deduce that

$$C_S k^{-2} \|(\boldsymbol{\delta_u}, \delta_p)\|_{\mathrm{DG}(h,k)}$$
$$\leq A'_{h,k}[\boldsymbol{u}_{H,K}](\boldsymbol{\delta_u}, \boldsymbol{v}) + B_{h,k}(\boldsymbol{v}, \delta_p) - B_{h,k}(\boldsymbol{\delta_u}, q)$$
$$= A'_{h,k}[\boldsymbol{u}_{H,K}](\boldsymbol{u}_{h,k} - \boldsymbol{u}_{H,K}, \boldsymbol{v}) + A'_{h,k}[\boldsymbol{u}_{H,K}](\boldsymbol{u}_{H,K} - \boldsymbol{u}_{2G}, \boldsymbol{v}) + B_{h,k}(\boldsymbol{v}, \delta_p)$$
$$= A'_{h,k}[\boldsymbol{u}_{H,K}](\boldsymbol{u}_{h,k} - \boldsymbol{u}_{H,K}, \boldsymbol{v}) + A_{h,k}(\boldsymbol{u}_{H,K}; \boldsymbol{u}_{H,K}, \boldsymbol{v}) - F_{h,k}(\boldsymbol{v}) + B_{h,k}(\boldsymbol{v}, p_{h,k})$$
$$= A'_{h,k}[\boldsymbol{u}_{H,K}](\boldsymbol{u}_{h,k} - \boldsymbol{u}_{H,K}, \boldsymbol{v}) + A_{h,k}(\boldsymbol{u}_{H,K}; \boldsymbol{u}_{H,K}, \boldsymbol{v}) - A_{h,k}(\boldsymbol{u}_{h,k}; \boldsymbol{u}_{h,k}, \boldsymbol{v})$$
$$= -\mathcal{Q}(\boldsymbol{u}_{H,K}, \boldsymbol{u}_{h,k}, \boldsymbol{v}).$$

Hence, employing Lemma 12 again gives

$$\|(\boldsymbol{u}_{h,k} - \boldsymbol{u}_{2G}, p_{h,k} - p_{2G})\|_{\mathrm{DG}(h,k)}$$
$$\leq C k^4 h^{-1} \left(1 + \|\underline{e}(\boldsymbol{u}_{h,k})\|_{L^\infty(\Omega)} + \|\underline{e}(\boldsymbol{u}_{H,K})\|_{L^\infty(\Omega)}\right) \|\boldsymbol{u}_{h,k} - \boldsymbol{u}_{H,K}\|_{h,k}^2 \|\boldsymbol{v}\|_{h,k}.$$

Applying Lemma 13, noting that $k \geq K \geq 1$, inequality (41) and the *a priori* error bound stated in Theorem 3, gives

$$\|(\boldsymbol{u}_{h,k} - \boldsymbol{u}_{2G}, p_{h,k} - p_{2G})\|_{\mathrm{DG}(h,k)}$$
$$\leq C \frac{k^{15/2}}{h} \left\{ \|\boldsymbol{u} - \boldsymbol{u}_{h,k}\|_{h,k}^2 + \|\boldsymbol{u} - \boldsymbol{u}_{H,K}\|_{h,k}^2 \right\}$$
$$\leq C \frac{k^{23/2}}{h} \left\{ \frac{h^{2r-2}}{k^{2s-3}} \|\boldsymbol{u}\|_{H^s(\Omega)}^2 + \frac{h^{2r-2}}{k^{2s-2}} \|p\|_{H^{s-1}(\Omega)}^2 + \frac{H^{2R-2}}{K^{2s-3}} \|\boldsymbol{u}\|_{H^s(\Omega)}^2 \right.$$
$$\left. + \frac{H^{2R-2}}{K^{2s-2}} \|p\|_{H^{s-1}(\Omega)}^2 \right\}.$$

Noting that $h \leq H$ and that $k \geq K$ completes the proof of the first bound (37). To prove the second bound (38), we first employ the triangle inequality

$$\|(\boldsymbol{u} - \boldsymbol{u}_{2G}, p - p_{2G})\|_{\mathrm{DG}(h,k)}$$
$$\leq \|(\boldsymbol{u} - \boldsymbol{u}_{h,k}, p - p_{h,k})\|_{\mathrm{DG}(h,k)} + \|(\boldsymbol{u}_{h,k} - \boldsymbol{u}_{2G}, p_{h,k} - p_{2G})\|_{\mathrm{DG}(h,k)}.$$

Thereby, applying the *a priori* error bound in Theorem 3, along with the bound (37) completes the proof of Theorem 10. $\qquad\square$

4.2. *A posteriori* error bound. In this section we state the following *a posteriori* upper bound for the numerical approximation defined by (33)–(36).

Theorem 14. *Let* $(\boldsymbol{u}, p) \in H_0^1(\Omega)^d \times L_0^2(\Omega)$ *be the analytical solution of* (1)–(3), $(\boldsymbol{u}_{H,K}, p_{H,K}) \in \boldsymbol{V}(\mathcal{T}_H, \boldsymbol{K}) \times Q(\mathcal{T}_H, \boldsymbol{K})$ *the numerical approximation obtained from* (33)–(34) *and* $(\boldsymbol{u}_{2G}, p_{2G}) \in \boldsymbol{V}(\mathcal{T}_h, \boldsymbol{k}) \times Q(\mathcal{T}_h, \boldsymbol{k})$ *the numerical approximation obtained from* (35)–(36)*; then the following hp-*a posteriori *error bound holds*

$$\|(\boldsymbol{u} - \boldsymbol{u}_{2G}, p - p_{2G})\|_{\mathrm{DG}(h,k)}$$

$$\leq C \left(\sum_{\kappa \in \mathcal{T}_h} \left(\eta_\kappa^2 + \xi_\kappa^2 \right) + \sum_{\kappa \in \mathcal{T}_h} h_\kappa^2 k_\kappa^{-2} \|\boldsymbol{f} - \Pi_{\kappa,k_\kappa} \boldsymbol{f}\|_{L^2(\kappa)}^2 \right)^{\frac{1}{2}},$$

with a constant $C > 0$*, which is independent of* $\boldsymbol{h}$, $\boldsymbol{H}$, $\boldsymbol{k}$, $\boldsymbol{K}$*. Here, for all* $\kappa \in \mathcal{T}_h$*, the* local fine grid error indicators η_κ *are defined by*

$$(42) \quad \eta_\kappa^2 = h_\kappa^2 k_\kappa^{-2} \|\Pi_{\kappa,k_\kappa} \boldsymbol{f} + \nabla \cdot \{\mu(|\underline{e}(\boldsymbol{u}_{H,K})|)\underline{e}(\boldsymbol{u}_{2G})\}\|_{L^2(\kappa)}^2 + \|\nabla \cdot \boldsymbol{u}_{2G}\|_{L^2(\kappa)}^2$$

$$+ h_\kappa k_\kappa^{-1} \left\| [\![p_{2G}]\!] - \underline{[\![\mu(|\underline{e}(\boldsymbol{u}_{H,K})|)\underline{e}(\boldsymbol{u}_{2G})]\!]} \right\|_{L^2(\partial\kappa \backslash \Gamma)}^2 + \gamma^2 h_\kappa^{-1} k_\kappa^3 \left\| [\![\boldsymbol{u}_{2G}]\!] \right\|_{L^2(\partial\kappa)}^2$$

and the local two-grid error indicators ξ_κ *are defined, for all* $\kappa \in \mathcal{T}_h$*, as*

$$(43) \quad \xi_\kappa^2 = \|(\mu(|\underline{e}(\boldsymbol{u}_{H,K})|) - \mu(|\underline{e}(\boldsymbol{u}_{2G})|))\underline{e}(\boldsymbol{u}_{2G})\|_{L^2(\kappa)}^2$$

$$+ \left\| \left(\mu'_{\underline{e}(u)}(|\underline{e}(\boldsymbol{u}_{H,K})|) : (\underline{e}(\boldsymbol{u}_{2G}) - \underline{e}(\boldsymbol{u}_{H,K})) \right) \underline{e}(\boldsymbol{u}_{H,K}) \right\|_{L^2(\kappa)}^2$$

$$+ h_F k_F^{-1} \left\| \left(\mu'_{\underline{e}(u)}(|\underline{e}(\boldsymbol{u}_{H,K})|) : (\underline{e}(\boldsymbol{u}_{2G}) - \underline{e}(\boldsymbol{u}_{H,K})) \right) \underline{e}(\boldsymbol{u}_{H,K}) \right\|_{L^2(\partial\kappa)}^2.$$

Proof. The proof of this theorem follows in an analogous manner to the proof of Theorem 6. We note that the *a posteriori* error bound for the two-grid method based on a single Newton iteration contains two extra terms in the local two-grid error indicators compared to the result derived in Theorem 6 for the two-grid approximation defined in (13)–(14). These two extra terms appear, trivially, from the bound of T_1 from (30), cf. [13], where instead of adding (9), with a specific $\boldsymbol{v}_{h,k}$, (35) has to be added instead. $\qquad\square$

5. *hp-***Adaptive Mesh Refinement**

For the standard IP DGFEM discretization of the non-Newtonian problem (1)–(3), cf. (9)–(10), the mesh and polynomial degree distribution may be automatically constructed using the *hp*-adaptive refinement algorithm outlined in [13]. In that setting, the local error indicators are defined in an analogous way to η_κ given in (22) or (42), for the two different two-grid methods, with $\boldsymbol{u}_{H,K}$ and $\boldsymbol{u}_{2G}$ both replaced by $\boldsymbol{u}_{h,k}$. In the context of the two-grid IP DGFEM discretizations defined by (13)–(16) and (33)–(36), it is necessary to refine both the fine and coarse meshes, together with their corresponding polynomial degrees, in order to decrease the error measured in the energy norm.

In [15] we proposed an algorithm that refined the fine mesh based only on η_κ and the coarse mesh based only on ξ_κ. In the current article we propose an alternative, more general purpose algorithm. In order to formally define this algorithm we first re-write the algorithm from [15] in the following form.

Algorithm 1. *The hp–finite element spaces* $\boldsymbol{V}(\mathcal{T}_h, \boldsymbol{k})$, $Q(\mathcal{T}_h, \boldsymbol{k})$, $\boldsymbol{V}(\mathcal{T}_H, \boldsymbol{K})$ *and* $Q(\mathcal{T}_H, \boldsymbol{K})$ *are constructed, based on employing the following algorithm.*

(0) *Initial step: Select initial coarse and fine meshes $\mathcal{T}_H$ and $\mathcal{T}_h$, respectively, as well as initial coarse and fine polynomial degree distributions $\boldsymbol{K}$ and $\boldsymbol{k}$, respectively, in such a manner that $\boldsymbol{V}(\mathcal{T}_H, \boldsymbol{K}) \subseteq \boldsymbol{V}(\mathcal{T}_h, \boldsymbol{k})$ and $Q(\mathcal{T}_H, \boldsymbol{K}) \subseteq Q(\mathcal{T}_h, \boldsymbol{k})$.*

(1) *Select elements in $\mathcal{T}_h$ and $\mathcal{T}_H$ for refinement/derefinement, based on the local fine grid error indicators η_κ and the two-grid local error indicators ξ_κ from $(22)/(42)$ and $(23)/(43)$, respectively.*

(2) *For elements marked for refinement in the fine and coarse mesh, determine whether to perform h- or p-refinement; see, for example, [20, 29].*

(3) *Perform mesh smoothing to ensure:*
   - *For all fine elements $\kappa \in \mathcal{T}_h$ there exists a coarse mesh element $\kappa_H \in \mathcal{T}_H$ such that $\kappa \subseteq \kappa_H$;*
   - *For all $\kappa \in \mathcal{T}_h$ and $\kappa_H \in \mathcal{T}_H$, where $\kappa \subseteq \kappa_H$, that $K_\kappa \leq k_\kappa$.*

   In this article we perform h-refinement on the fine mesh $\mathcal{T}_h$ and p-derefinement on the coarse mesh $\mathcal{T}_H$ where necessary.

Remark 4. For the purposes of the numerical experiments in the following section, in Step 0 above, the two-grid hp-adaptive algorithm is initially started with $\boldsymbol{V}(\mathcal{T}_H, \boldsymbol{K}) = \boldsymbol{V}(\mathcal{T}_h, \boldsymbol{k})$ and $Q(\mathcal{T}_H, \boldsymbol{K}) = Q(\mathcal{T}_h, \boldsymbol{k})$.

In order to employ this algorithm we need a strategy to select elements in $\mathcal{T}_h$ and $\mathcal{T}_H$ for refinement/derefinement, cf. Step 1 above. In this paper we propose an algorithm based on first identifying regions to refine using $\eta_\kappa + \xi_\kappa$ and then selecting the mesh to refine dependent on which of the two error indicators is dominant.

Algorithm 2. *Elements in the coarse and fine meshes $\mathcal{T}_H$ and $\mathcal{T}_h$, respectively, are selected for refinement/derefinement based on employing the following algorithm.*

(1) *Determine the sets $\mathfrak{R}(\mathcal{T}_h) \subseteq \mathcal{T}_h$ and $\mathfrak{D}(\mathcal{T}_h) \subseteq \mathcal{T}_h$ of fine elements to be (potentially) refined/derefined, respectively, based on the size of $\eta_\kappa + \xi_\kappa$ using a standard refinement algorithm, e.g., the fixed fraction refinement strategy.*

(2) *For all elements selected for derefinement decide whether to perform derefinement of the fine or coarse mesh: for all $\kappa \in \mathfrak{D}(\mathcal{T}_h)$*
   - *if $\lambda_F \xi_\kappa \leq \eta_\kappa$ derefine the coarse element $\kappa_H \in \mathcal{T}_H$, where $\kappa \subseteq \kappa_H$, and*
   - *if $\lambda_C \eta_\kappa \leq \xi_\kappa$ derefine the fine element κ.*

(3) *For all elements selected for refinement decide whether to perform refinement of the fine or coarse mesh: for all $\kappa \in \mathfrak{R}(\mathcal{T}_h)$*
   - *if $\lambda_F \xi_\kappa \leq \eta_\kappa$ refine the fine element κ and*
   - *if $\lambda_C \eta_\kappa \leq \xi_\kappa$ refine the coarse element $\kappa_H \in \mathcal{T}_H$, where $\kappa \subseteq \kappa_H$.*

Here, $\lambda_F, \lambda_C \in (0, \infty)$ are steering parameters selected such that $\lambda_F \lambda_C \leq 1$.

Remark 5. We note that it is possible that a coarse element $\kappa_H \in \mathcal{T}_H$ could be marked for both refinement and derefinement. When this occurs the coarse element is refined, as refinement should take precedence over derefinement.

Proposition 15. *For all elements $\kappa \in \mathfrak{R}(\mathcal{T}_h)$ either the fine element $\kappa \in \mathcal{T}_h$ or the coarse element $\kappa_H \in \mathcal{T}_H$, where $\kappa \subseteq \kappa_H$, will be marked for refinement.*

Proof. To prove this statement it is sufficient to show that either $p(\kappa) : \lambda_F \xi_\kappa \leq \eta_\kappa$ or $q(\kappa) : \lambda_C \eta_\kappa \leq \xi_\kappa$ is true for all $\kappa \in \mathcal{T}_h$. For any $\kappa \in \mathcal{T}_h$, if $p(\kappa)$ is true then $p(\kappa) \vee q(\kappa)$ is true by definition; hence, it is only necessary to prove that $q(\kappa)$ is
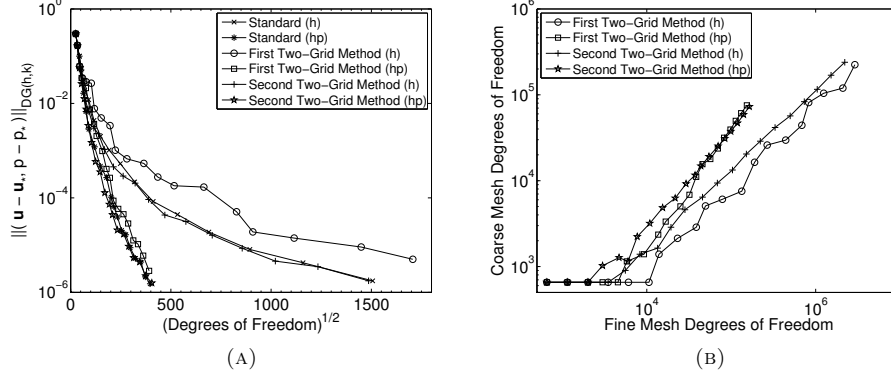
FIGURE 1. Example 1. (a) Comparison of the error in the DG norm, using the standard ($\boldsymbol{u}_* = \boldsymbol{u}_{h,k}$, $p_* = p_{h,k}$) and both two-grid methods ($\boldsymbol{u}_* = \boldsymbol{u}_{2G}$, $p_* = p_{2G}$), with respect to the number of degrees of freedom; (b) Comparison of number of degrees of freedom in the coarse and fine mesh.

true if $p(\kappa)$ is false. As $q(\kappa)$ is false and $\lambda_F \lambda_C \leq 1$ then

$$\lambda_F \xi_\kappa > \eta_\kappa \geq \lambda_F \lambda_C \eta_\kappa.$$

Dividing through by $\lambda_F > 0$ gives that $\xi_\kappa \geq \lambda_C \eta_\kappa$; hence, $q(\kappa)$ is true if $p(\kappa)$ is false. □

Remark 6. We note that although a similar result exists for the derefinement of elements $\kappa \in \mathfrak{D}(\mathcal{T}_h)$ it is possible for no element to be derefined for an element $\kappa \in \mathfrak{D}(\mathcal{T}_h)$ due to Remark 5.

6. Numerical Experiments

In this section we perform a series of numerical experiments to demonstrate the performance of the *a posteriori* error bounds derived in Theorems 6 and 14 within the automatic hp-adaptive mesh refinement procedure based on one-irregular quadrilateral elements for $\Omega \subset \mathbb{R}^2$ defined in Section 5. Throughout this section the two-grid IP DGFEM solutions obtained by (13)–(16) and (33)–(36) are calculated with $\theta = 0$. We additionally set the constant γ arising in the interior penalty parameter $\sigma_{h,k}$ defined by (11) to 10. The resulting system of nonlinear equations, on the coarse mesh, are solved based on employing a damped Newton method; for each inner (linear) iteration, as well as the linear fine mesh system, we employ the MUMPS Solver, see [1, 2, 3].

The mesh adaptation is undertaken based on employing Algorithm 1 with the decision concerning whether to refine coarse or fine meshes, Step 1, based on utilising Algorithm 2 with steering parameters $\lambda_C = 1/2$ and $\lambda_F = 1$. The selection of regions to refine, Step 1 of Algorithm 2, is achieved via a fixed fraction strategy where the refinement and derefinement fractions are set to 25% and 5%, respectively. We employ the hp-adaptive strategy developed by [20] to decide whether to perform h- or p-refinement/derefinement in Step 2 of Algorithm 1. We note here that we start with a polynomial degree of $k_{\kappa_h} = 3$ for all $\kappa_h \in \mathcal{T}_h$ and $K_{\kappa_H} = 3$
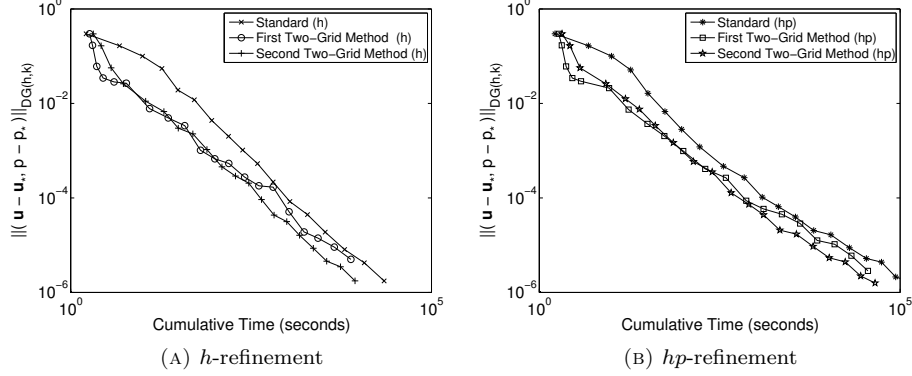
FIGURE 2. Example 1. Cumulative CPU timing of the standard $(\boldsymbol{u}_* = \boldsymbol{u}_{h,k}, p_* = p_{h,k})$ and both two-grid $(\boldsymbol{u}_* = \boldsymbol{u}_{2G}, p_* = p_{2G})$ solvers compared to the error in the DG norm.
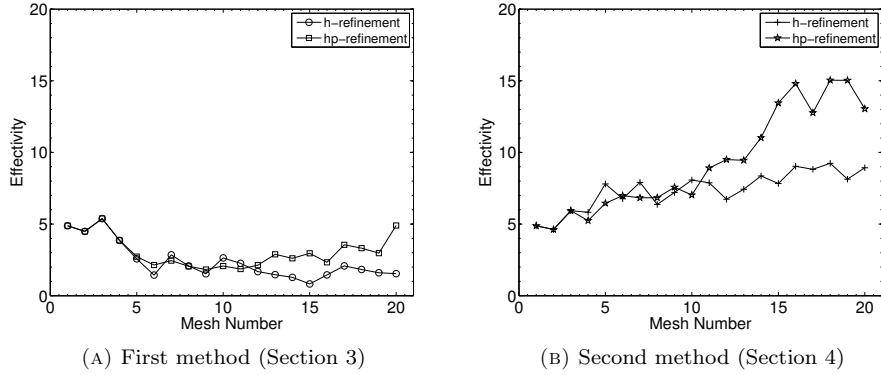

FIGURE 3. Example 1. Effectivity of the h- and hp-refinement using both two-grid methods.

for all $\kappa_H \in \mathcal{T}_H$. For each example, as well as solving using both two-grid IP DGFEMs, we compute the standard IP DGFEM formulation (9), (10) for comparison. In addition to hp-refinement, we also compute the numerical solution using all three discretization methods with an h-adaptive refinement strategy, using the same 25% and 5% refinement/derefinement fixed fraction strategy, with a fixed (uniform) polynomial degree distribution; for h-refinement, we set $\lambda_C = 1$.

6.1. Example 1: Smooth solution. In this example we consider the cavity-like problem from [7, Section 6.1] using the Carreau law nonlinearity

$$(44) \qquad \mu(|\underline{e}(\boldsymbol{u})|) = k_\infty + (k_0 - k_\infty)(1 + \lambda_c |\underline{e}(\boldsymbol{u})|^2)^{(\vartheta-2)/2},$$
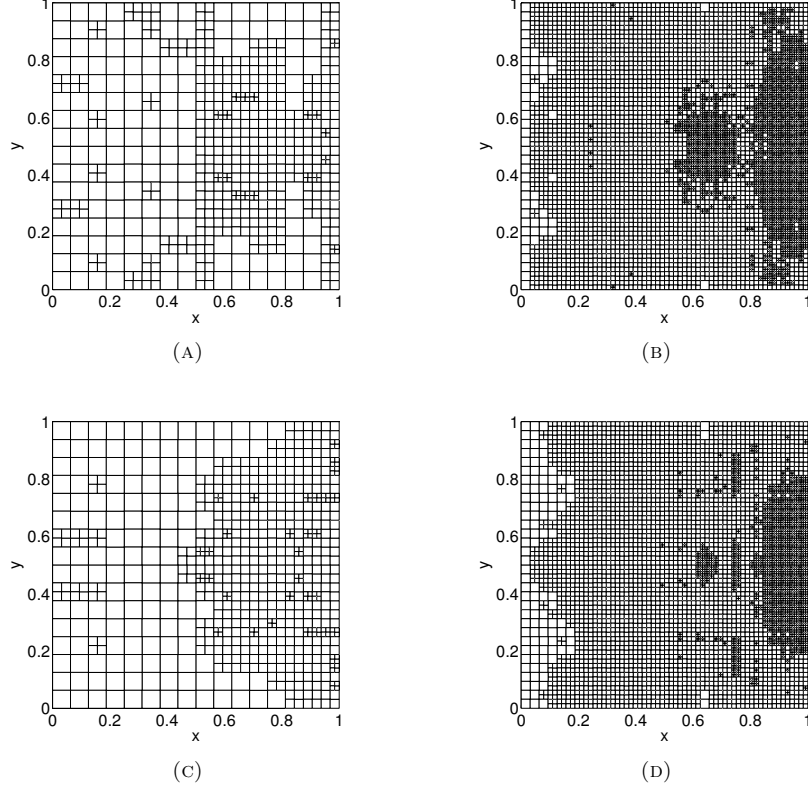
FIGURE 4. Example 1. Coarse and fine mesh after 13 h-adaptive mesh refinements: (a) & (b) Coarse and fine mesh, respectively, for first two-grid method (Section 3); (c) & (d) Coarse and fine mesh, respectively, for second two-grid method (Section 4)

with $k_\infty = 0$, $k_0 = 2$, $\lambda_c = 1$ and $\vartheta = 1.2$. We let $\Omega = (0,1)^2$ be the unit square and select the forcing function $\boldsymbol{f}$ such that the analytical solution to (1)–(3) is given by

$$(45) \qquad \boldsymbol{u}(x,y) = \begin{pmatrix} \left(1 - \cos\left(2\frac{\pi\left(e^{\vartheta x}-1\right)}{e^\vartheta-1}\right)\right)\sin(2\pi y) \\ -\vartheta e^{\vartheta x}\sin\left(2\frac{\pi\left(e^{\vartheta x}-1\right)}{e^\vartheta-1}\right)\frac{1-\cos(2\pi y)}{e^\vartheta-1} \end{pmatrix},$$

$$(46) \qquad p(x,y) = 2\pi\vartheta e^{\vartheta x}\sin\left(2\frac{\pi\left(e^{\vartheta x}-1\right)}{e^\vartheta-1}\right)\frac{\sin(2\pi y)}{e^\vartheta-1}.$$

In Figure 1(a) we present a comparison of the true error, measured in the DGFEM norm $\|(\cdot,\cdot)\|_{DG(h,k)}$, of the standard and two-grid IP DGFEMs with the square root of the number of the degrees of freedom (of the fine mesh) on a linear-log scale for both h- and hp-adaptive mesh refinement algorithms. Here, we can see that the true error stemming from using the two-grid IP DGFEM based on a single Newton iteration (the second two-grid method) is similar to the corresponding
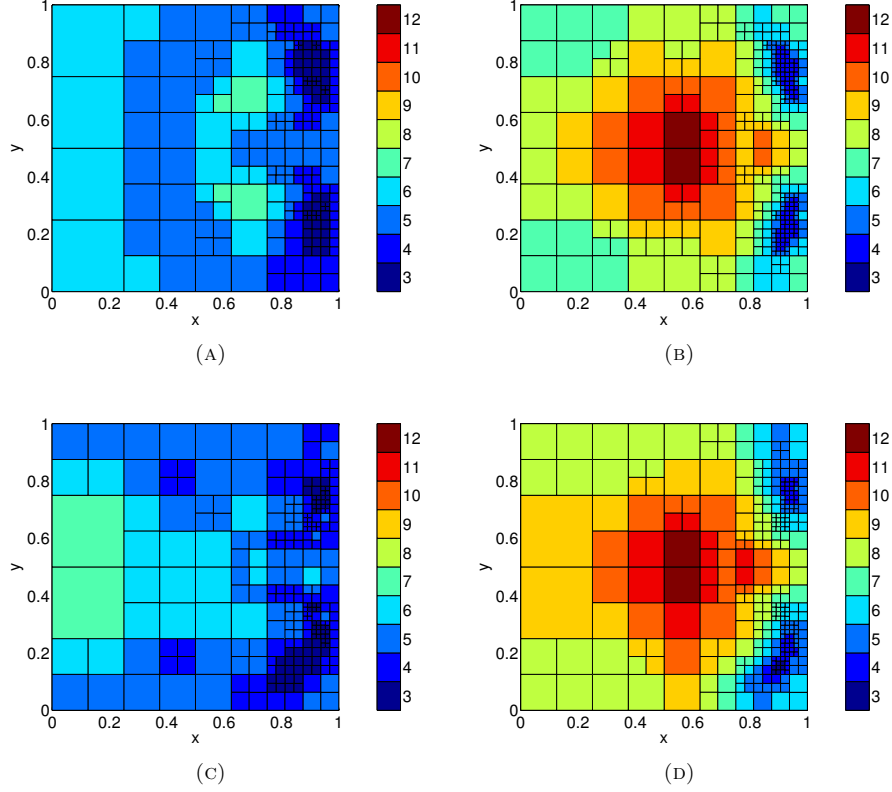
FIGURE 5. Example 1. Coarse and fine mesh after 13 hp-adaptive
mesh refinements: (a) & (b) Coarse and fine mesh, respectively,
for first two-grid method (Section 3); (c) & (d) Coarse and fine
mesh, respectively, for second two-grid method (Section 4)

quantity computed for the standard IP DGFEM, for a given number of degrees of
freedom in the two-grid fine mesh as in the standard IP DGFEM mesh; in contrast,
the first two-grid method is notable inferior for h-refinement. In Figure 1(b) we
plot the number of degrees of freedom in the coarse mesh compared to the number
in the fine mesh for both two-grid methods; here we observe that there are consid-
erable less degrees of freedom in the coarse finite element space than the fine one,
as we would expect. The comparison of the true error, measured in the DGFEM
norm, of the standard and two-grid IP DGFEMs with respect to the cumulative
computation time, in seconds, on a log-log scale for both h- and hp-adaptive mesh
refinement algorithms is shown in Figure 2. As can be seen for both strategies the
two-grid methods result in the same true error for a lower computation time, when
compared to the standard (single-grid) IP DGFEM. The second two-grid method
based on a single Newton iteration appears to perform slightly better than the first
two-grid method in terms of computation time reduction. From Figure 3 we see
that for both the h- and hp-refinement strategies that the *a posteriori* error bound
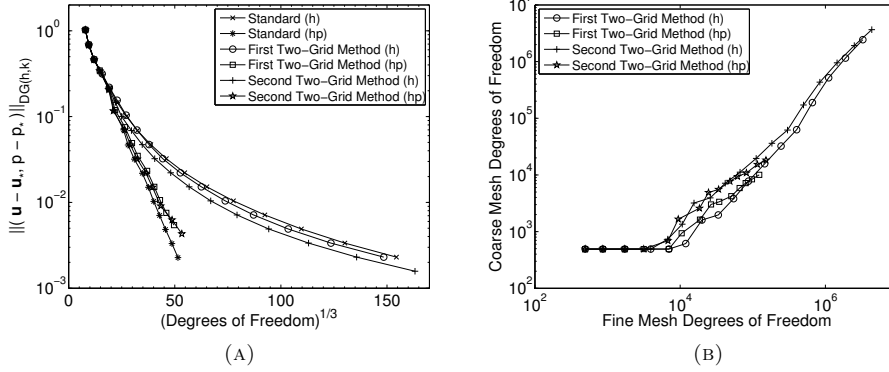for both the two-grid IP DGFEMs overestimates the true error by a consistent

FIGURE 6. Example 2. (a) Comparison of the error in the DG norm, using the standard ($\boldsymbol{u}_* = \boldsymbol{u}_{h,k}$, $p_* = p_{h,k}$) and both two-grid methods ($\boldsymbol{u}_* = \boldsymbol{u}_{2G}$, $p_* = p_{2G}$), with respect to the number of degrees of freedom; (b) Comparison of number of degrees of freedom in the coarse and fine mesh.

amount in the sense that the effectivity indices are roughly constant for all meshes; we point out that the second two-grid method based on a single Newton iteration gives rise to a slightly higher effectivity index for hp-refinement.

In Figure 4 we show the coarse and fine meshes for both two-grid IP DGFEMs after 13 h-mesh refinements. We note that the coarse and fine mesh appear to be refined in roughly the same manner, but with less refinement in the coarse mesh. We can also see that the second two-grid IP DGFEM based on a single Newton iteration has resulted in slightly more coarse refinement and less fine refinement. Figure 5 shows the coarse and fine meshes after 13 hp-mesh refinements. Here, the h-refinements have occurred mostly around the interior of the hills and valleys of the pressure with p-refinement in the rest of the domain which is largely smooth, as would be expected from a smooth analytical solution, with the highest p-refinement being around the vortex centre at the point $(1/\vartheta \log((e^\vartheta+1)/2), 1/2)$. We note here that the two different two-grid methods have broadly refined in a similar manner, the most noticeable difference being on the coarse mesh.

6.2. Example 2: Singular solution. For this example we consider a nonlinear version of the singular solution from [28, p. 113], see also [18], using the nonlinearity

$$\mu(|\underline{e}(\boldsymbol{u})|) = 1 + e^{-|\underline{e}(\boldsymbol{u})|}.$$

We let Ω be the L-shaped domain $(-1,1)^2 \setminus [0,1) \times (-1,0]$ and select $\boldsymbol{f}$ so that the analytical solution to (1)–(3), where (r,φ) denotes the system of polar coordinates, is given by

$$\boldsymbol{u}(r,\varphi) = r_s^\lambda \left(\begin{array}{c} (1+\lambda_s)\sin(\varphi)\Psi(\varphi) + \cos(\varphi)\Psi'(\varphi) \\ \sin(\varphi)\Psi'(\varphi) - (1+\lambda_s)\cos(\varphi)\Psi(\varphi) \end{array} \right),$$

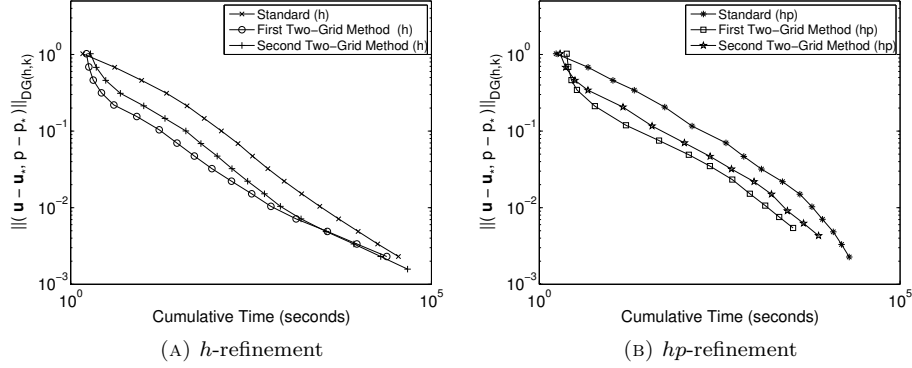$$p(r,\varphi) = -r^{\lambda_s-1} \frac{(1+\lambda_s)^2\Psi'(\varphi) + \Psi'''(\varphi)}{1-\lambda_s},$$

Figure 7. Example 2. Cumulative CPU timing of the standard $(\boldsymbol{u}_* = \boldsymbol{u}_{h,k}, p_* = p_{h,k})$ and both two-grid $(\boldsymbol{u}_* = \boldsymbol{u}_{2G}, p_* = p_{2G})$ solvers compared to the error in the DG norm.
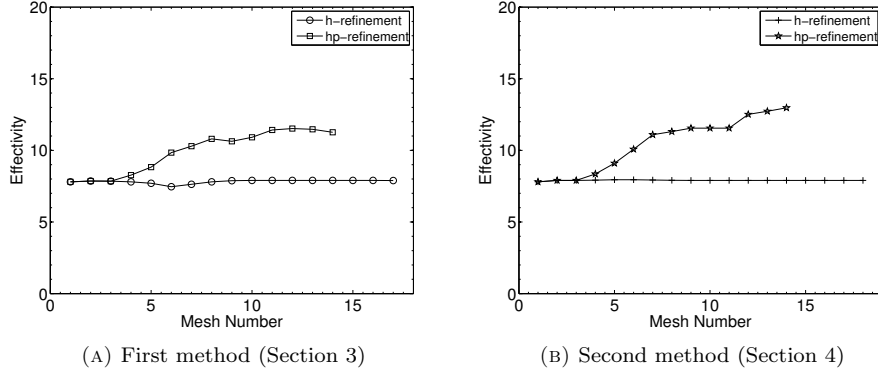

Figure 8. Example 2. Effectivity of the h- and hp-refinement using both two-grid methods.

where

$$\Psi(\varphi) = \frac{\sin((1 + \lambda_s)\varphi)\cos(\lambda_s\omega)}{1 + \lambda_s} - \cos((1 + \lambda_s)\varphi)$$
$$- \frac{\sin((1 - \lambda_s)\varphi)\cos(\lambda_s\omega)}{1 - \lambda_s} + \cos((1 - \lambda_s)\varphi),$$

and $\omega = \frac{3\pi}{2}$. Here, the exponent λ_s is the smallest positive solution of

$$\sin(\lambda_s\omega) + \lambda_s\sin(\omega) = 0;$$

thereby, $\lambda_s \approx 0.54448373678246$.

We again compare in Figure 6(a) the true error, measured in the DGFEM norm, of the standard and two-grid IP DGFEMs with respect to the third root of the degrees of freedom (of the fine mesh) on a linear-log scale for both adaptive mesh
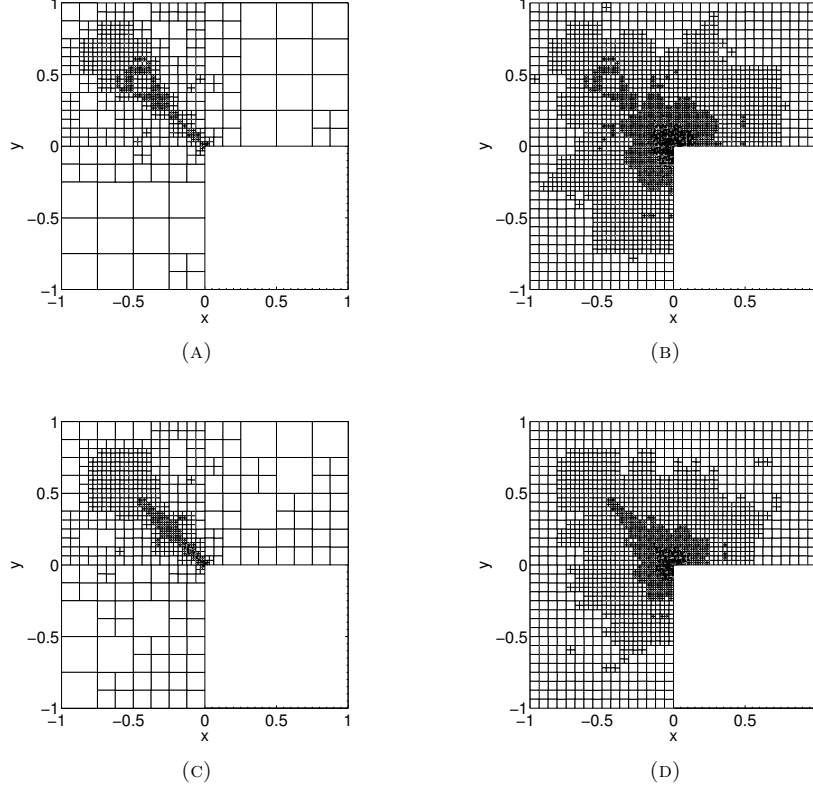
FIGURE 9. Example 2. Coarse and fine mesh after 11 h-adaptive mesh refinements: (a) & (b) Coarse and fine mesh, respectively, for first two-grid method (Section 3); (c) & (d) Coarse and fine mesh, respectively, for second two-grid method (Section 4)

refinement algorithms. We notice that the error in the DGFEM norm for the two-grid IP DGFEMs is roughly the same as the error in the DGFEM norm for the standard IP DGFEM, when employing the same number of degrees of freedom in the fine mesh as in the mesh for the standard IP DGFEM. Figure 6(b) compares the number of degrees of freedom in the two meshes for both two-grid methods. Both two-grid methods appear to have similar numbers of degrees of freedom in the coarse and fine meshes as each other. We also note that, although initially the number of degrees of freedom in the coarse meshes for h-refinement are considerably less than in the fine meshes, as refinement continues the number of degrees of freedom in the coarse and fine meshes converge. As before we are interested in the performance improvement that is attained by undertaking the two-grid IP DGFEMs as opposed to the standard IP DGFEM; therefore, in Figure 7 the true error, measured in the DGFEM norm, of the standard and two-grid IP DGFEMs is compared to the cumulative computation time, in seconds, on a log-log scale for both h- and hp-adaptive mesh refinement algorithms. We note that a computational time improvement is seen for both the h- and hp-adaptive two-grid IP
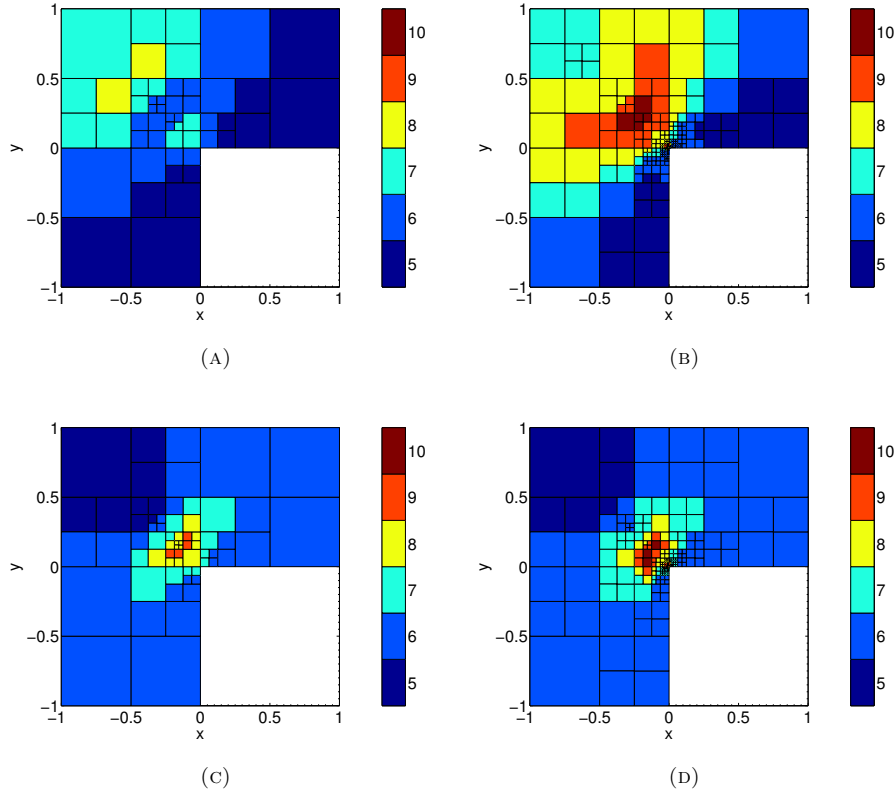
FIGURE 10. Example 2. Coarse and fine mesh after 11 hp-adaptive mesh refinements: (a) & (b) Coarse and fine mesh, respectively, for first two-grid method (Section 3); (c) & (d) Coarse and fine mesh, respectively, for second two-grid method (Section 4)

DGFEMs compared to the standard IP DGFEM. Unlike in the smooth problem the second two-grid method based on a single Newton iteration appears to perform slightly worse than the first two-grid method in terms of computation time reduction. Figure 8 illustrates that, for both the h- and hp-refinement strategy, that the effectivity constants are roughly constant indicating that the *a posteriori* error bound for both two-grid IP DGFEMs overestimates the true error by roughly a constant; indeed for the h-adaptive refinement it is almost exactly 8 for all meshes. For the hp-adaptive refinement the effectivity indices does rise initially before becoming constant at around 12 for the first two-grid method and rising slightly more in the second two-grid method based on a single Newton iteration.

We show the coarse and fine meshes for both two-grid IP DGFEMs after 11 h- and hp-adaptive mesh refinements in Figure 9 and Figure 10, respectively. For h-adaptive refinement we note that the focus of the refinement in the fine mesh is in the vicinity of the singularity at the origin; however, in the coarse mesh, refinement is undertaken in the region near both the singularity and the line $y = -x$ coming from the singularity, where it appears that the coarse mesh needs to be almost as

refined as the fine mesh. This behaviour is also demonstrated with hp-adaptive mesh refinement, although less noticeable, for the first two-grid method. The two methods have resulted in notably different hp-refinements with the second two-grid method undertaking very minimal refinement along the line $y = -x$.

7. Concluding remarks

In this article we have extended the *a priori* and *a posteriori* analysis developed in [13], for hp-version interior penalty discontinuous Galerkin methods for the discretization of quasi-Newtonian fluid flow problems, to the two-grid setting. In particular, we have studied two variants of the two-grid IP DGFEM: one is based on committing a modelling/data approximation error on the fine finite element mesh, while the second approach is based on utilizing a single step of a Newton iterative solver. The latter method yields improved *a priori* error bounds, in the sense that, to attain optimal convergence of the underlying method, the coarse finite element space may be less refined than for the former approach. However, when conducting hp-adaptive mesh refinement, we observe that the two discretization methods yield very similar convergence behaviour. We also note that the reduction in computational time between utilizing the two-grid methods proposed in this article for a quasi-Newtonian fluid flow problem, in comparison to the employing the standard IP DGFEM, is quite modest for the simple numerical test cases computed in this article. We point out that this is in part due to the exploitation of the very efficient MUMPS direct solver for the solution of the underlying linear systems of equations; for larger problems, which require the use of iterative methods, such as preconditioned GMRES, for example, typically two-grid methods are computationally much more efficient than employing standard single grid techniques; cf. [11, 15], for example. Additionally, two-grid methods possess a number of very attractive features. Indeed, the numerical approximation of nonlinear problems on fine finite element partitions can be very computationally expensive; for more challenging problems than those considered in this article, it is not guaranteed that a nonlinear solver will converge as the complexity, i.e., the number of degrees of freedom in the underlying finite element space, increases. Hence, approximating the nonlinear problem only on a coarser mesh, where, for example, a (damped) Newton solver can be exploited to efficiently compute a coarse solution, followed by the solution of only a linear problem on the desired fine mesh, potentially yields a more robust solver. Finally, since two-grid methods naturally employ two embedded finite element spaces, the solution of the underlying linear problem on the finest finite element space naturally lends itself to the exploitation of domain decomposition preconditioners. This latter issue, together with the analysis of two-grid methods for more general nonlinearities than those studied in this article, forms the basis of our future work.

Acknowledgments

References

[1] P. R. Amestoy, I. S. Duff, J. Koster, and J.-Y. L'Excellent. A fully asynchronous multifrontal solver using distributed dynamic scheduling. *SIAM J. Matrix Anal. Appl.*, 23(1):15–41, 2001.
[2] P. R. Amestoy, I. S. Duff, and J.-Y. L'Excellent. Multifrontal parallel distributed symmetric and unsymmetric solvers. *Comput. Methods Appl. Mech. Engrg.*, 184:501–520, 2000.

[3] P. R. Amestoy, A. Guermouche, J.-Y. L'Excellent, and S. Pralet. Hybrid scheduling for the parallel solution of linear systems. *Parallel Comput.*, 32(2):136–156, 2006.

[4] O. Axelsson and W. Layton. A two-level method for the discretization of nonlinear boundary value problems. *SIAM J. Numer. Anal.*, 33(6):2359–2374, 1996.

[5] O. Axelsson and W. Layton. A two-level method for the discretization of nonlinear boundary value problems. *SIAM J. Numer. Anal.*, 33(6):2359–2374, 1996.

[6] I. Babuška and M. Suri. The $h - p$ version of the finite element method with quasiuniform meshes. *RAIRO Modél. Math. Anal. Numér.*, 21(2):199–238, 1987.

[7] S. Berrone and E. Süli. Two-sided a posteriori error bounds for incompressible quasi-Newtonian flows. *IMA J. Numer. Anal.*, 28:382–421, 2008.

[8] C. Bi and V. Ginting. Two-grid finite volume element method for linear and nonlinear elliptic problems. *Numer. Math.*, 108:177–198, 2007.

[9] C. Bi and V. Ginting. Two-grid discontinuous Galerkin method for quasi-linear elliptic problems. *J. Sci. Comput.*, 49(3):311–331, 2011.

[10] F. Brezzi and M. Fortin. *Mixed and Hybrid Finite Element Methods*. Springer Series in Computational Mathematics. Springer-Verlag, New York, 1991.

[11] S. Congreve. *Two-Grid hp-Version Discontinuous Galerkin Finite Element Methods for Quasilinear PDEs*. PhD thesis, University of Nottingham, submitted.

[12] S. Congreve and P. Houston. Two-grid *hp*-DGFEM for second order quasilinear elliptic PDEs based on an incomplete Newton iteration. In J. Li, H. Yang, and E. Machorro, editors, *Proceedings of the 8th International Conference on Scientific Computing and Applications*, volume 586 of *Contemporary Mathematics*, pages 135–142. AMS, 2013.

[13] S. Congreve, P. Houston, E. Süli, and T. P. Wihler. *hp*-version discontinuous Galerkin finite element methods for strongly monotone quasi-Newtonian flows. *IMA J. Numer. Anal.*, In press.

[14] S. Congreve, P. Houston, and T. P. Wihler. Two-grid *hp*-version DGFEMs for strongly monotone second-order quasilinear elliptic PDEs. In G. Brenn, G. Holzapfel, M. Schanz, and O. Steinbach, editors, *Proceedings in Applied Mathematics and Mechanics. 82nd Annual GAMM Scientific Conference, Graz, Austria*, volume 11, pages 3–6, 2011.

[15] S. Congreve, P. Houston, and T. P. Wihler. Two-grid *hp*-version discontinuous Galerkin finite element methods for second-order quasilinear elliptic PDEs. *J. Sci. Comput.*, 55(2):471–497, 2013.

[16] C. N. Dawson, M. F. Wheeler, and C. S. Woodward. A two-grid finite difference scheme for non-linear parabolic equations. *SIAM J. Numer. Anal.*, 35:435–452, 1998.

[17] P. Hansbo and M. G. Larson. Discontinuous Galerkin methods for incompressible and nearly incompressible elasticity by Nitsche's method. *Comput. Methods Appl. Mech. Engrg.*, 191(17–18):1895–1908, 2002.

[18] P. Houston, D. Schötzau, and T. P. Wihler. *hp*-adaptive discontinuous Galerkin finite element methods for the Stokes problem. In P. Neittaanmäki, T. Rossi, S. Korotov, J. Périaux, and D. Knörzer, editors, *Proc. of the European Congress on Computational Methods in Applied Sciences and Engineering*, volume II, 2004.

[19] P. Houston, D. Schötzau, and T. P. Wihler. Energy norm a-posteriori error estimation of *hp*-adaptive discontinuous Galerkin methods for elliptic problems. *Math. Models Methods Appl. Sci.*, 17:33–62, 2007.

[20] P. Houston and E. Süli. A note on the design of *hp*-adaptive finite element methods for elliptic partial differential equations. *Comput. Methods Appl. Mech. Engrg.*, 194(2–5):229–243, 2005.

[21] P. Houston, E. Süli, and T. P. Wihler. A posteriori error analysis of *hp*-version discontinuous Galerkin finite-element methods for second-order quasi-linear PDEs. *IMA J. Numer. Anal.*, 28(2):245–273, 2008.

[22] O. A. Karakashian and F. Pascal. A posteriori error estimates for a discontinuous Galerkin approximation of second-order elliptic problems. *SIAM J. Numer. Anal.*, 41(6):2374–2399, 2003.

[23] M. Marion and J. Xu. Error estimates on a new nonlinear Galerkin method based on two-grid finite elements. *SIAM J. Numer. Anal.*, 32(4):1170–1184, 1995.

[24] D. Schötzau, C. Schwab, and A. Toselli. Mixed *hp*-DGFEM for incompressible flows. *SIAM J. Numer. Anal.*, 40(6):2171–2194, 2002.

[25] C. Schwab. *p- and hp-FEM — Theory and Applications in Solid and Fluid Mechanics*. Oxford University Press, Oxford, 1998.

[26] A. Toselli. *hp* discontinuous Galerkin approximations for the Stokes problem. *Math. Models Methods Appl. Sci.*, 12(11):1565–1597, 2002.

[27] T. Utnes. Two-grid finite element formulations of the incompressible Navier–Stokes equations. *Comm. Numer. Meth. Engng.*, 13(8):675–684, 1997.

[28] R. Verfürth. *A review of a posteriori error estimation and adaptive mesh-refinement techniques.* Teubner, 1996.

[29] T. P. Wihler. An *hp*-adaptive strategy based on continuous Sobolev embeddings. *J. Comput. Appl. Math.*, 235(8):2731–2739, 2011.

[30] L. Wu and M. Allen. Two-grid method for mixed finite-element solution of coupled reaction-diffusion systems. *Numerical Methods for Partial Differential Equations*, 1999:589–604, 1999.

[31] J. Xu. A new class of iterative methods for nonselfadjoint or indefinite problems. *SIAM J. Numer. Anal.*, 29:303–319, 1992.

[32] J. Xu. A novel two-grid method for semilinear elliptic equations. *SIAM J. Sci. Comp.*, 15:231–237, 1994.

[33] J. Xu. Two-grid discretization techniques for linear and nonlinear PDEs. *SIAM J. Numer. Anal.*, 33(5):1759–1777, 1996.

[34] L. Zhu, S. Giani, P. Houston, and D. Schötzau. Energy norm a posteriori error estimation for *hp*-adaptive discontinuous Galerkin methods for elliptic problems in three dimensions. *Math. Models Methods Appl. Sci.*, 21(2):267–306, 2011.

[35] L. Zhu and D. Schötzau. A robust a posteriori error estimate for *hp*-adaptive DG methods for convection-diffusion equations. *IMA J. Numer. Anal.*, 31(3):971–1005, 2010.

Mathematisches Institut, Universität Bern, Sidlerstrasse 5, CH-3012 Bern, Switzerland
E-mail: `scott.congreve@math.unibe.ch`

School of Mathematical Sciences, University of Nottingham, University Park, Nottingham NG7 2RD, UK.
E-mail: `paul.houston@nottingham.ac.uk`